Geophysical Journal International

Geophys. J. Int. (2014) **197,** 1770–1788
Advance Access publication 2014 April 17

doi: 10.1093/gji/ggu088

On estimating attenuation from the amplitude of the spectrally whitened ambient seismic field

Cornelis Weemstra,[1,2] Willem Westra,[3] Roel Snieder[4] and Lapo Boschi[5,6]

[1] *Spectraseis, Denver, CO, USA. E-mail: kweemstra@gmail.com*
[2] *Institute of Geophysics, ETH, Sonneggstrasse 5, CH-8092 Zürich, Switzerland*
[3] *Department of Mathematics, University of Iceland - Dunhaga 3, 107 Reykjavik, Iceland*
[4] *Center for Wave Phenomena, Colorado School of Mines, Golden, CO 80401, USA*
[5] *UPMC, Université Paris 06, ISTEP, F-75005 Paris, France*
[6] *CNRS, UMR 7193, F-75005, Paris, France*

Accepted 2014 March 7. Received 2014 March 7; in original form 2013 July 18

SUMMARY

Measuring attenuation on the basis of interferometric, receiver–receiver surface waves is a non-trivial task: the amplitude, more than the phase, of ensemble-averaged cross-correlations is strongly affected by non-uniformities in the ambient wavefield. In addition, ambient noise data are typically pre-processed in ways that affect the amplitude itself. Some authors have recently attempted to measure attenuation in receiver–receiver cross-correlations obtained after the usual pre-processing of seismic ambient-noise records, including, most notably, spectral whitening. Spectral whitening replaces the cross-spectrum with a unit amplitude spectrum. It is generally assumed that cross-terms have cancelled each other prior to spectral whitening. Cross-terms are peaks in the cross-correlation due to simultaneously acting noise sources, that is, spurious traveltime delays due to constructive interference of signal coming from different sources. Cancellation of these cross-terms is a requirement for the successful retrieval of interferometric receiver–receiver signal and results from ensemble averaging. In practice, ensemble averaging is replaced by integrating over sufficiently long time or averaging over several cross-correlation windows. Contrary to the general assumption, we show in this study that cross-terms are not required to cancel each other prior to spectral whitening, but may also cancel each other after the whitening procedure. Specifically, we derive an analytic approximation for the amplitude difference associated with the reversed order of cancellation and normalization. Our approximation shows that an amplitude decrease results from the reversed order. This decrease is predominantly non-linear at small receiver–receiver distances: at distances smaller than approximately two wavelengths, whitening prior to ensemble averaging causes a significantly stronger decay of the cross-spectrum.

Key words: Interferometry; Surface waves and free oscillations; Seismic attenuation.

GJI Seismology

1 INTRODUCTION

Over the last decade the research field of ambient seismic noise has flourished. Its success in geophysics dates back to the derivation of Claerbout (1968), who relates the transmission response of a horizontally layered medium to the reflection response of the same medium. He later generalized his theory to the cross-correlation of noise recorded at two locations making an analogous conjecture for the 3-D Earth (Rickett & Claerbout 1999). The response that is retrieved by cross-correlating two receiver recordings can therefore be interpreted as the response that would be measured at one of the receiver locations as if there were a source at the other. This is now known as passive seismic interferometry (SI) and its first successful application in seismology is due to Campillo & Paul (2003). The technique is successfully applied to other media than the Earth: among others, solar seismology (Duvall *et al.* 1993), underwater acoustics (Roux & Fink 2003), ultrasonics (Weaver & Lobkis 2001, 2002), retrieving the building response (Snieder & Åžafak 2006; Kohler *et al.* 2007) and infrasound (Haney 2009).

While Campillo & Paul (2003) used earthquake coda to extract empirical Green's functions (EGFs), Shapiro & Campillo (2004) showed that broad-band Rayleigh waves emerge by simple cross-correlation of continuous recordings of ambient seismic noise. These surface waves can be used for velocity inversion on a continental scale (e.g. Shapiro *et al.* 2005; Yang *et al.* 2007) as well as on a local scale (e.g. Brenguier *et al.* 2007; Bussat & Kugler 2009). More recently, it has been shown that, under certain circumstances and for specific locations and bandwidths, also body waves can be

retrieved from the ambient seismic wavefield (e.g. Draganov *et al.* 2007, 2009; Nakata *et al.* 2011; Poli *et al.* 2012; Lin *et al.* 2013).

Much attention has been paid to the pre-processing of data, which includes spectral whitening and time-domain normalization (Bensen *et al.* 2007). Time-domain normalization involves a variety of methods to remove earthquake signals and instrumental irregularities from the recordings. Such events interrupt the stationarity of time-series. The first successful applications employed the so-called one-bit normalization (Campillo & Paul 2003; Larose *et al.* 2004; Shapiro & Campillo 2004), while later studies used more involved time-domain normalization techniques (e.g. Sabra *et al.* 2005; Yang *et al.* 2007). Whitening of the spectra prior to cross-correlation, without any time-domain normalization, turns out to be very effective (Brenguier *et al.* 2007; Prieto *et al.* 2009; Lawrence & Prieto 2011; Verbeke *et al.* 2012). Recently, Seats *et al.* (2012) have shown that spectral whitening alone gives a faster convergence to year-long EGFs than spectral whitening combined with running normalization or one-bit normalization.

In recent years, several researchers have focused on estimating attenuation based on interferometric measurements of surface waves (Prieto *et al.* 2009; Lawrence & Prieto 2011; Weemstra *et al.* 2013). The methodology is based on the derivation of the normalized spatial autocorrelation (SPAC) by Aki (1957). He showed that, given a stationary wavefield over a laterally homogenous medium, the normalized azimuthally averaged cross-spectrum coincides with a Bessel function of the first kind of order zero (henceforth Bessel function). A large amount of literature discussing the SPAC can be found (e.g. Chávez-García *et al.* 2005; Asten 2006) and an extensive review is given by Okada (2003). Nakahara (2012) formulates the SPAC method in dissipative media for 1-, 2- and 3-D scalar wavefields. The relation between the SPAC on one hand and SI on the other hand is shown by Yokoi & Margaryan (2008) and Tsai & Moschetti (2010).

The studies of Prieto *et al.* (2009), Lawrence & Prieto (2011) and Weemstra *et al.* (2013) estimate subsurface attenuation by fitting a damped Bessel function to the real part of the azimuthally averaged coherency. The azimuthally averaged coherency varies as a function of distance for individual frequencies. This leads to an estimation of the quality factor, Q, as a function of frequency. The obtained Q-values are indicative of the depth variation of attenuation and correlate with the geology in the survey area (Prieto *et al.* 2009; Lawrence & Prieto 2011; Weemstra *et al.* 2013). It should be noted that, despite these results, it is now well understood that the distribution of noise sources has a significant effect on the behaviour of the azimuthally averaged coherency (Tsai 2011; Weaver 2012).

An apparent inconsistency arises from the study of Weemstra *et al.* (2013): they require the real part of the azimuthally averaged coherency to be fit by a downscaled version of the damped Bessel function instead of a damped Bessel function with a value of 1 at zero distance. That is, the damped Bessel function coincides with the real part of the azimuthally averaged coherency up to a proportionality constant. The objective of this study is to explain this inconsistency, that is, the required proportionality constant. This factor is not predicted by theory (e.g. Aki 1957; Tsai 2011), which suggests that either one (or more) of the assumptions made in these theoretical studies is violated by Weemstra *et al.* (2013) or that the theory is simply wrong. The first suggestion is correct: we show in this study that the inconsistency observed by Weemstra *et al.* (2013) can be explained by the employed normalization procedure in the cross-correlation, whitening and stacking process.

A commonly made assumption in SI studies is that noise sources are uncorrelated. This assumption implies that 'cross-terms', that is peaks in the cross-correlation originating from simultaneously acting noise sources, cancel after ensemble-averaging (e.g. Aki 1957; Snieder 2004; Tsai 2011; Wapenaar *et al.* 2011; Hanasoge 2013). Mathematically (e.g. Wapenaar *et al.* 2010), this cancellation can be written as $\langle N_j(t) * N_k(-t)\rangle = \delta_{jk}[N_j(t) * N_k(-t)]$, where δ_{jk} is the Kronecker delta function, $\langle . \rangle$ denotes ensemble averaging and $N_j(t)$ is the noise produced by a noise source at $\boldsymbol{x}_j$. The asterisk denotes temporal convolution, but the time reversal of the second noise series turns this into a cross-correlation. Given uncorrelated noise sources, ensemble averaging on one hand and cancellation of cross-terms on the other hand are therefore closely related; in fact, the latter is the result of the former. Ensemble averages can be taken over time, azimuth or a combination of these. In all cases, however, averaging needs to be sufficient for cross-terms to cancel out.

In practice, cross-correlations are often computed in the frequency domain: noise recordings are Fourier transformed and the spectrum at one station is multiplied by the complex conjugate of the spectrum at another station. Spectral whitening involves an additional step where the amplitude of the obtained cross-spectrum is set to unity for all frequencies. Ensemble averaging, combined with spectral whitening, yields the complex coherency computed in the attenuation studies mentioned above (Prieto *et al.* 2009; Lawrence & Prieto 2011; Weemstra *et al.* 2013). In this paper, we show that the behaviour of the coherency as a function of distance depends on the order of these two procedures: spectral normalization of individual cross-spectra prior to averaging yields a lower amplitude coherency than spectral normalization after ensemble averaging. This lower amplitude can be attributed to the involvement of cross-terms in the normalization procedure. Specifically, we find that the amplitude decrease is non-linear, which results in an excess decay of the coherency at small receiver separations. Our results suggest that the normalization procedure employed by Weemstra *et al.* (2013) included cross-terms.

We use the model introduced by Tsai (2011) to evaluate the difference between spectral whitening after cancellation of the cross-terms and whitening prior to cancellation of the cross-terms. After introduction of this model (Section 2), we derive an expression for the two just mentioned cases (Section 3). Finally, we verify the obtained analytical expressions numerically (Section 4).

2 CROSS-CORRELATIONS IN AN AMBIENT SEISMIC FIELD

We start with the definition of the time-domain cross-correlation C_{xy}: for recordings $u_T(\boldsymbol{x})$ and $u_T(\boldsymbol{y})$, captured at surface locations $\boldsymbol{x}$ and $\boldsymbol{y}$,

$$C^T_{xy}(t) \equiv \frac{1}{2T}\int_{-T}^{T} u_T(\boldsymbol{x},\tau)u_T(\boldsymbol{y},\tau+t)\,\mathrm{d}\tau, \tag{1}$$

where t is time, τ is integration time and where we have normalized with respect to the length of the employed cross-correlation window, that is, T. We assume the length of this cross-correlation window to be sufficiently long with respect to the longest period within the frequency range of interest, that is, $T \gg 1/\omega$, with ω the angular frequency. In case of monochromatic signal oscillating with angular frequency ω this implies that the term that includes the 'sinc' function can be neglected (see e.g. eq. 6 of Tsai & Moschetti 2010). We define the frequency domain cross-correlation, that is,

the cross-spectrum as $\hat{C}^T_{xy}(\omega) \equiv \mathbb{F}[C^T_{xy}(t)]$, where $\mathbb{F}$ is the temporal Fourier transform.

We will now describe how the displacement at the surface due to ambient vibrations can be written as a sum over sources. This description is similar to the model introduced by Tsai (2011). Because we allow for attenuation, we base our discussion on the damped wave equation:

$$\frac{1}{c^2}\frac{\partial^2 u}{\partial t^2} + \frac{2\alpha}{c}\frac{\partial u}{\partial t} = \nabla^2 u. \tag{2}$$

Ocean microseisms, the main source of ambient seismic noise on the Earth, excite surface waves much more effectively than all other seismic phases; we therefore apply (2) to an elastic membrane (Peter *et al.* 2007), interpreting u as any single-mode displacement, for example, Rayleigh waves. We assume $c(\omega)$ and $\alpha(\omega)$ to be laterally invariant (or sufficiently smooth as to such that an approximate solution can be obtained). The Green's function associated with the 2-D damped wave equation is approximated, for a single frequency, by (Tsai 2011),

$$\begin{aligned} G^{(0)}(\boldsymbol{x};\boldsymbol{s},\omega) &= \frac{\mathrm{i}}{4} H_0\left(\frac{r_{sx}\omega}{c}\sqrt{1+\frac{2\mathrm{i}\alpha c}{\omega}}\right) \\ &\approx \frac{\mathrm{i}}{4} H_0\left(\frac{r_{sx}\omega}{c}\right)\mathrm{e}^{-\alpha r_{sx}}, \end{aligned} \tag{3}$$

where the approximation holds for weak attenuation, that is, $\omega/c \gg \alpha$. H_0 is a zero-order Hankel function of the first kind (henceforth Hankel function) and $r_{sx} \equiv |\boldsymbol{s}-\boldsymbol{x}|$ is the distance from the source ($\boldsymbol{s}$) to the receiver ($\boldsymbol{x}$). Note that both c and α may change as a function of ω, but that we drop this dependency in the expressions for simplicity. Alternatively, the constraint on the attenuation can be written in the form $2\pi/\lambda \gg \alpha$, where λ denotes the wavelength and relates to the phase velocity and angular frequency as $\lambda = 2\pi c/\omega$.

We consider the displacement at $\boldsymbol{x}$ due to N sources. Each source's signal is described by a cosine oscillating with an angular frequency ω_0 and amplitude A, but with a different random phase ϕ_j; the subscript refers to the source. The randomness of the phases implies that we assume uncorrelated sources. Assuming each source to be oscillating for a period of T_a seconds, the Fourier transform of its signal is computed in Appendix A; we refer to T_a as the 'realization time'. We write the total displacement at $\boldsymbol{x}$ due to sources at $\boldsymbol{s}_j$, where $j = 1,\ldots,N$, by

$$\begin{aligned} \hat{u}(\boldsymbol{x},\omega) &= \sum_{j=1}^{N} \hat{S}_j(\omega)\,\mathrm{e}^{\mathrm{i}\phi_j}\,G^{(0)}(\boldsymbol{x};\boldsymbol{s}_j,\omega) \\ &= \frac{\mathrm{i}}{4}\sum_{j=1}^{N} \hat{S}_j(\omega)\mathrm{e}^{\mathrm{i}\phi_j} H_0\left(\frac{r_{jx}\omega}{c}\right)\mathrm{e}^{-\alpha r_{jx}}, \end{aligned} \tag{4}$$

where the amplitude due to the source at $\boldsymbol{s}_j$ is denoted by $\hat{S}_j(\omega)$, its phase by ϕ_j and the distance between that source and the receiver by r_{jx}. We assume the phases ϕ_j to be random variables homogeneously distributed between 0 and 2π. Note that $\hat{S}_j$ includes the amplitude spectrum associated with the Fourier transformation of the random phase cosine, that is,

$$\hat{S}_j(\omega) = \frac{A_j T_a\ \mathrm{sinc}\left[(\omega_0-\omega)\,T_a/2\right]}{2\sqrt{2\pi}}, \tag{5}$$

where A_j is the actual amplitude of the source. Although the source only oscillates at a single frequency ω_0, spectral leakage occurs due to the finite nature of its signal. This leakage is captured by the sinc function. Note that this is different from the analysis performed by Tsai (2011), who considers the cross-spectrum of the limiting case, $T_a \to \infty$. Furthermore, we note that site amplification is ignored, but could be accounted for by multiplying the right-hand side of eq. (4) with an extra function of $\boldsymbol{x}$ and ω (Tsai 2011).

The displacement at $\boldsymbol{x}$ may also consist of non-propagating noise, that is, noise that is local to $\boldsymbol{x}$ and hence is not accounted for by the damped wave equation. This non-propagating noise could be due to local environmental sources (see e.g. Olofsson 2010) or instrument noise (e.g. Sleeman *et al.* 2006; Ringler & Hutt 2010). It can be incorporated by adding a term to eq. (4) which describes its amplitude and phase (Tsai 2011). We neglect this non-propagating noise however. This assumption might not be valid for frequencies for which the ambient field has little power, but may be a reasonable assumption for frequencies in the range of the microseismic peaks (e.g. Peterson 1993; McNamara & Buland 2004; Sleeman *et al.* 2006; Ringler & Hutt 2010).

The displacement model of eq. (4) enables us to derive expressions for the cross-correlation and autocorrelations associated with a single 'source correlation time'. The source correlation time gives the time required for the phase of a noise source's signal to become uncorrelated with the phase of the signal emitted by that same source at an earlier time. Our model's analogue to source correlation time is realization time and, accordingly, phases ϕ_j are referred to as 'realizations'. By definition, then, the phase ϕ_j of a source at $\boldsymbol{s}_j$ changes randomly between realizations. Note that T_a may be frequency dependent and, also, may change from one source (region) to another. For simplicity, however, we assume all sources to have equal realization times. The power of a source is assumed constant between realizations.

For simplification, we first isolate the source phases in eq. (4) and write the displacement associated with a single realization at x as,

$$\hat{u}(\boldsymbol{x},\omega) = \sum_{j=1}^{N} f_{jx}\mathrm{e}^{\mathrm{i}\phi_j}, \tag{6}$$

with the phase independent part described by f_{jx}, that is,

$$f_{jx}(\omega) \equiv \frac{\mathrm{i}}{4}\hat{S}_j(\omega)H_0\left(\frac{r_{jx}\omega}{c}\right)\mathrm{e}^{-\alpha r_{jx}}. \tag{7}$$

The frequency dependence of f_{jx} is henceforth omitted because we only consider a single frequency.

We calculate the cross-spectrum for a single realization and frequency ω,

$$\begin{aligned} \hat{C}_{xy} &= \hat{u}(\boldsymbol{x})\hat{u}^*(\boldsymbol{y}) \\ &= \left(\sum_{j=1}^{N} f_{jx}\mathrm{e}^{\mathrm{i}\phi_j}\right)\times\left(\sum_{k=1}^{N} f^*_{ky}\mathrm{e}^{-\mathrm{i}\phi_k}\right) \\ &= \sum_{j=1}^{N}\sum_{k=1}^{N} f_{jx}f^*_{ky}\mathrm{e}^{\mathrm{i}\phi_j-\phi_k}, \end{aligned} \tag{8}$$

where the complex conjugate of a variable z is denoted z^*. Note that we explicitly omit the superscript T since this cross-correlation is computed over T_a. This sum can be split in two summations: one sum over N cross-correlations of signal associated with the N sources and another sum over $N(N-1)$ cross-correlations of signal associated with different sources. The latter sum is over the so-called 'cross-terms' (explained in more detail by Wapenaar *et al.* 2010). Splitting eq. (8) gives

$$\hat{C}_{xy} = \sum_{j=1}^{N} f_{jx}f^*_{jy} + \sum_{j=1}^{N}\sum_{k\neq j} f_{jx}f^*_{ky}\mathrm{e}^{\mathrm{i}(\phi_j-\phi_k)}. \tag{9}$$

The first summation does not depend on the phases of the sources and hence does not differ from one realization to the other. We will refer to this term as the 'coherent term' and it will be denoted by $\hat{C}_{xyC}$, that is,

$$\hat{C}_{xyC} \equiv \sum_{j=1}^{N} f_{jx} f_{jy}^{*}. \tag{10}$$

The second summation however, does change from one realization to the other. Each of the cross-terms in this summation has a different random phase and, also, a different amplitude. Consequently, this summation will result in a random walk of $N(N-1)$ different sized steps in the complex plane. We will refer to this term as the 'incoherent term' and it will be denoted $\hat{C}_{xyI}$, that is,

$$\hat{C}_{xyI} \equiv \sum_{j=1}^{N} \sum_{k \neq j} f_{jx} f_{ky}^{*} \mathrm{e}^{\mathrm{i}(\phi_j - \phi_k)}. \tag{11}$$

We now consider the Fourier decomposition of the displacement associated with a cross-correlation window of length T, that is, $\mathbb{F}[u_T]$, denoted by $\hat{u}_T$. The frequency-domain source displacement over a time window of length T, with T coinciding with a total of M realization times ($T \equiv M \times T_a$), is simply a sum of the displacements associated with the individual realizations, that is, individual $\hat{u}$ (see Appendix A). Note that we, for simplicity, assume T an integer multiple of T_a. The displacement at x over a cross-correlation window of length T can then be written as

$$\hat{u}_T(\boldsymbol{x}, \omega) = \sum_{p=1}^{M} \sum_{j=1}^{N} f_{jx} h_p \mathrm{e}^{\mathrm{i}\phi_{jp}}, \tag{12}$$

where ϕ_{jp} is the phase of the signal emitted by source j in the p-th realization. Further, the term $h_p(\omega) \equiv \mathrm{e}^{\mathrm{i}(\omega_0 - \omega)(pT_a - T_a/2)}$, accounts for the phase shift originating from the difference in onset between the p-th realization and the cross-correlation window (see Appendix A). Recall that in our formulation different realizations are analogous to different time windows of length T_a where source phases are assumed to have changed (randomly) from one time window to the next and that source amplitudes are assumed constant between realizations. Using this frequency-domain expression for the displacement, the cross-correlation defined in eq. (1) is, for a single frequency, obtained by

$$\begin{aligned} \hat{C}_{xy}^{T}(\omega) &= \hat{u}_T(\boldsymbol{x}) \hat{u}_T^{*}(\boldsymbol{y}) \\ &= \sum_{p=1}^{M} \sum_{q=1}^{M} \sum_{j=1}^{N} \sum_{k=1}^{N} f_{jx} f_{ky}^{*} h_p h_q^{*} \mathrm{e}^{\mathrm{i}(\phi_{jp} - \phi_{kq})}. \end{aligned} \tag{13}$$

We can write $\hat{C}_{xy}^{T}$ in terms of the coherent term defined in eq. (10) and an incoherent term associated with $\hat{C}_{xy}^{T}$, that is,

$$\hat{C}_{xy}^{T}(\omega) = M \left(\hat{C}_{xyC} + \hat{C}_{xyI}^{T} \right), \tag{14}$$

where $\hat{C}_{xyI}^{T}$ is given by

$$\begin{aligned} \hat{C}_{xyI}^{T} \equiv \frac{1}{M} \sum_{p=1}^{M} \sum_{q \neq p} \sum_{j=1}^{N} f_{jx} f_{jy}^{*} h_p h_q^{*} \mathrm{e}^{\mathrm{i}(\phi_{jp} - \phi_{jq})} \\ + \frac{1}{M} \sum_{p=1}^{M} \sum_{q=1}^{M} \sum_{j=1}^{N} \sum_{k \neq j} f_{jx} f_{ky}^{*} h_p h_q^{*} \mathrm{e}^{\mathrm{i}(\phi_{jp} - \phi_{kq})}. \end{aligned} \tag{15}$$

In the decomposition of $\hat{C}_{xy}^{T}$ we use the fact that the elements for which $j = k$ and $p = q$ are independent of the random source phases, whereas the other elements, captured in $\hat{C}_{xyI}^{T}$, remain dependent on these phases. Similarly, $\hat{C}_{xxI}^{T}$ and $\hat{C}_{yyI}^{T}$ are given by the right-hand side of eq. (15) with y replaced by x and x by y, respectively.

Note that eq. (14) suggests that averaging over long time, instead of over many different time windows, does not make cross-terms disappear: both the coherent term and incoherent term of $\hat{C}_{xy}^{T}$, that is, $M\hat{C}_{xyC}$ and $M\hat{C}_{xyI}^{T}$, respectively, grow linearly with M. Here it should be understood that the $1/M$ factor included in $\hat{C}_{xyI}^{T}$ is balanced by a factor M arising from the 2-D random walk of M^2 steps associated with the double sum over the M^2 random phases. Since T scales linearly with M, this implies that increasing the length of the cross-correlation window does not render the cross-terms of $\hat{C}_{xy}^{T}$ negligible. This perhaps surprising behaviour is discussed in more detail at the end of Section 3.

3 SPECTRAL WHITENING AND ENSEMBLE AVERAGING

A frequently made assumption in SI studies is one of mutually uncorrelated noise sources (e.g. Aki 1957; Snieder 2004; Wapenaar *et al.* 2011; Hanasoge 2013). This assumption implies that cross-terms, that is, $\hat{C}_{xyI}^{T}$ in our formulation, cancel after ensemble averaging. In our framework, the ensemble average is defined as

$$\left\langle C_{xy}^{T} \right\rangle \equiv \frac{1}{W} \sum_{v=1}^{W} C_{xy_v}^{T}, \tag{16}$$

where W is the number of computed cross-correlations and each $C_{xy_v}^{T}$ is a different cross-correlation, that is, a cross-correlation associated with a different moment in time.

By means of the model introduced in the last section, we will now evaluate the relation between (i) the employed cross-correlation window T, (ii) the realization time T_a and (iii) the spectral whitening procedure. Specifically, we focus on two end-member cases. The first is dubbed the 'whitened averaged coherency' and assumes that cross-terms have vanished prior to spectral whitening. The second we dub the 'averaged whitened coherency' and assumes that normalization takes place while the cross-terms are still present in the cross-spectrum. Note, however, that in both cases cross-terms eventually cancel each other out in the stacking process; it is simply the order of cancellation and normalization that is reversed.

3.1 Whitened averaged coherency

The whitened averaged coherency between recordings captured at surface locations $\boldsymbol{x}$ and $\boldsymbol{y}$ is defined as

$$\rho(\boldsymbol{x}, \boldsymbol{y}, \omega) \equiv \frac{\left\langle \hat{C}_{xy}^{T}(\omega) \right\rangle}{\sqrt{\left\langle \hat{C}_{xx}^{T}(\omega) \right\rangle} \sqrt{\left\langle \hat{C}_{yy}^{T}(\omega) \right\rangle}}. \tag{17}$$

Note that local (site) amplification at the receivers, due to medium inhomogeneities, is corrected for by this normalization (Okada 2003; Weaver 2012). This is because any such amplification would be present in both the numerator and denominator of (17).

The azimuthal average, denoted $Av[\ldots]$, is computed using all $\boldsymbol{x}$ and $\boldsymbol{y}$ for which $|\boldsymbol{x} - \boldsymbol{y}| = r$. The azimuthal average of ρ we denote $\bar{\rho}$. If we assume a spatially and temporally stochastic wavefield over a loss-less medium, we get (Okada 2003; Aki 1957),

$$\bar{\rho}(r, \omega) \equiv Av\left[\rho(\boldsymbol{x}, \boldsymbol{y}, \omega)\right] = J_0\left(\frac{r\omega}{c(\omega)}\right), \tag{18}$$

where J_0 denotes the 0-th order Bessel function of the first kind and $c(\omega)$ the wave velocity as a function of angular frequency (which implies that c is assumed to be independent of the surface locations $\boldsymbol{x}$ and $\boldsymbol{y}$). It is useful to note that in case of a uniform illumination of the receivers at $\boldsymbol{x}$ and $\boldsymbol{y}$, that is, an isotropic wavefield, $\rho(\boldsymbol{x}, \boldsymbol{y}, \omega)$ coincides with a Bessel function for any orientation of the line connecting the receivers at $\boldsymbol{x}$ and $\boldsymbol{y}$ (Tsai 2011).

Tsai (2011) shows how ρ behaves in the presence of attenuation, that is, a lossy instead of a loss-less medium, and finds that the source distribution strongly determines its rate of decay with distance. He shows for a number of source distributions how the real part of ρ behaves as a function of distance for a laterally invariant $c(\omega)$ and attenuation (we explicitly mention 'laterally invariant', because phase velocity and attenuation may still vary as a function of depth). He proves mathematically that for small $\alpha(\omega)$ and for a homogeneous distribution of sources that

$$\Re\left[\rho(r,\omega)\right] = J_0\left(\frac{r\omega}{c(\omega)}\right)\mathrm{e}^{-\alpha(\omega)r}, \tag{19}$$

where attenuation is included through multiplication of J_0 with an exponential factor $\mathrm{e}^{-\alpha(\omega)r}$ and where the operator $\Re[\ldots]$ maps its complex argument into its real part. The attenuation coefficient $\alpha(\omega)$ accounts for a more rapid decrease of the Bessel function with inter-receiver distance r and hence the effect of energy dissipation and scattering. Importantly, the imaginary component of $\rho(r, \omega)$ is zero for such a distribution of sources.

Calculation of ρ involves computation of the ensemble averages of $\hat{C}^T_{xy}$, $\hat{C}^T_{xx}$ and $\hat{C}^T_{xx}$ individually. Tsai (2011) implicitly assumes $T = T_a$, that is, $M = 1$, in eq. (13), and evaluates the ensemble average of $\hat{C}_{xy}$. He concludes that the cross-terms in expression (9) can be neglected in the limit of infinite realizations. More explicitly, he assumes two random walks associated with the ensemble average of C_{xyI}: one where the steps are associated with different realizations and the other the earlier mentioned random walk associated with the cross-terms. Due to the correlation between cross-terms $f_{jx}f^*_{ky}\mathrm{e}^{\mathrm{i}(\phi_j-\phi_k)}$ and $f_{kx}f^*_{jy}\mathrm{e}^{\mathrm{i}(\phi_k-\phi_j)}$ this random walk will be a so-called 'biased random walk' however. Because of this and because we do not necessarily require $T = T_a$, we choose a different approach than Tsai (2011) to evaluate the ensemble average of $\hat{C}^T_{xy}$.

We define the source phases ϕ_{jp} in eq. (13) to be random variables that are independent and identically distributed (i.i.d.) and described by a uniform distribution between 0 and 2π. The cross-correlation $\hat{C}^T_{xy}$ therefore depends on $N \times M$ random variables and hence $\hat{C}^T_{xy}$ is a random variable itself. These phases are the only variables in eq. (13) that vary between the different cross-correlation windows. Substituting (13) in (16), the ensemble average of $\hat{C}^T_{xy}$ is therefore given by

$$\left\langle \hat{C}^T_{xy} \right\rangle = \frac{1}{W}\sum_{v=1}^{W}\sum_{p=1}^{M}\sum_{q=1}^{M}\sum_{j=1}^{N}\sum_{k=1}^{N} f_{jx}f^*_{ky}h_p h^*_q \mathrm{e}^{\mathrm{i}(\phi_{jpv}-\phi_{kqv})}, \tag{20}$$

where ϕ_{jpv} is the phase of source j for realization p within cross-correlation window v.

For large W, the ensemble average of $\hat{C}^T_{xy}$ will tend to its expected value. Since we assume the phases to be independent identically distributed random variables, the expected value of the cross-correlation, denoted $E[\hat{C}^T_{xy}]$, can be computed by integrating eq. (14) from 0 to 2π over $\phi_{11}, \phi_{12}, \ldots, \phi_{1M}, \ldots, \phi_{N1}, \ldots, \phi_{NM}$. To reduce notational burden, we refer to this series of $N \times M$ random variables by $\phi^{N,M}$. The expected value is computed,

$$\begin{aligned} E\left[\hat{C}^T_{xy}\right] &= \frac{1}{(2\pi)^{N\times M}}\int_0^{2\pi}\hat{C}^T_{xy}(\phi^{N,M})\,\mathrm{d}\phi^{N,M} \\ &= M\hat{C}_{xyC} + \frac{1}{(2\pi)^{N\times M}}\int_0^{2\pi}\sum_{p=1}^{M}\sum_{q\neq p}\sum_{j=1}^{N} f_{jx}f^*_{jy}h_p h^*_q \mathrm{e}^{\mathrm{i}(\phi_{jp}-\phi_{jq})} \\ &\quad + \sum_{p=1}^{M}\sum_{q=1}^{M}\sum_{j=1}^{N}\sum_{k\neq j} f_{jx}f^*_{ky}h_p h^*_q \mathrm{e}^{\mathrm{i}(\phi_{jp}-\phi_{kq})}\,\mathrm{d}\phi^{N,M}. \end{aligned} \tag{21}$$

Because the integrands in eq. (21) traverse a circle in the complex plane from 0 to 2π, integration yields zero for these elements. Consequently, we find that cross-terms indeed vanish and that only the coherent term $\hat{C}_{xyC}$, multiplied by M, survives. Similarly, the expected values of the autocorrelations $\hat{C}^T_{xx}$ and $\hat{C}^T_{yy}$ coincide with $M \times \hat{C}_{xxC}$ and $M \times \hat{C}_{yyC}$, respectively. We therefore conclude, in agreement with Tsai (2011), that,

$$\rho(\boldsymbol{x}, \boldsymbol{y}, \omega) = \frac{\hat{C}_{xyC}}{\sqrt{\hat{C}_{xxC}\,\hat{C}_{yyC}}}. \tag{22}$$

Tsai (2011) shows how the source distribution determines the decay of the real part of this identity with distance between $\boldsymbol{x}$ and $\boldsymbol{y}$. For a number of specific (end-member) examples he explicitly computes this decay.

It should be understood that the fact that the expected value of $\hat{C}^T_{xy}$ coincides with $M\hat{C}_{xyC}$ for any value of M does not imply that its convergence towards $M\hat{C}_{xyC}$ is equally fast for any value of M. In fact, the expected fluctuations associated with $\hat{C}^T_{xyI}$ scale linearly with M because the expected absolute distance covered by a 2-D random walk of M^2 steps coincides with M. Consequently, for larger M, it may well be that more averaging is required to converge to $M\hat{C}_{xyC}$.

3.2 Averaged whitened coherency

We will now evaluate the effect of spectral whitening of the cross-spectrum prior to cancellation of the cross-terms. We denote this by γ and in the context of our model it is defined as

$$\gamma(\boldsymbol{x}, \boldsymbol{y}, \omega, T) \equiv \left\langle \frac{\hat{C}^T_{xy}(\omega)}{\sqrt{\hat{C}^T_{xx}(\omega)}\sqrt{\hat{C}^T_{yy}(\omega)}} \right\rangle. \tag{23}$$

Note that this expression coincides with $\langle \hat{C}_{xy}/|\hat{C}_{xy}| \rangle$ in case $M = 1$. Clearly, from a model perspective, γ is different from ρ. Because we aim to explain the proportionality constant required in the study of Weemstra *et al.* (2013), we briefly put the difference between γ and ρ in the context of their results.

Weemstra *et al.* (2013) employed cross-correlation windows with a length of 60 s. Discrete Fourier transforms (DFTs) of these noise series were computed for all stations and cross-correlation windows. For each individual station pair and cross-correlation window, the spectrally whitened cross-spectrum was computed by multiplication of the spectrum associated with the first station with the complex conjugate of the spectrum associated with the second station and subsequent normalization. For each discrete frequency, the coherency was obtained by subsequent averaging of the normalized cross-spectra over different cross-correlation windows. This procedure implies that their results should be interpreted as γ. We anticipate on the final result of this section by introducing the azimuthally averaged averaged whitened coherency, denoted $\bar{\gamma}$. Similarly as for the whitened averaged coherency, it is defined as

$\bar{\gamma}(r,\omega) \equiv Av[\gamma(\boldsymbol{x},\boldsymbol{y},\omega)]$ and averaging is over all $\boldsymbol{x}$ and $\boldsymbol{y}$ for which $|\boldsymbol{x}-\boldsymbol{y}| = r$. The results of the data analysis by Weemstra *et al.* (2013) indicate that

$$\Re[\bar{\gamma}(r,\omega)] = P(\omega)J_0\left(\frac{r\omega}{c(\omega)}\right)\mathrm{e}^{-\alpha(\omega)r}, \tag{24}$$

where $P(\omega)$ is a frequency-dependent proportionality factor. That is to say, other than (19), they require multiplication of the damped Bessel function with a proportionality constant.

We note that the coherency formulated and computed by Prieto *et al.* (2009) and Lawrence & Prieto (2011) differs from both ρ and γ. That is, in these studies cross-spectra are normalized with respect to the smoothed power-spectral densities at x and y. These narrow-bandwidth averages of individual $\hat{C}^T_{xx}(\omega)$ and $\hat{C}^T_{yy}(\omega)$ may well approximate the respective expected values, that is, $\hat{C}_{xxC}$ and $\hat{C}_{yyC}$, at the centre frequencies of these bandwidths to a fair degree. Consequently, the results obtained by these researchers may be explained better by the behaviour of ρ than by that of γ. This is discussed in more detail at the end of this section and in Section 5. We now turn to solving for γ analytically.

Similar to the ensemble average of $\hat{C}^T_{xy}$, the ensemble average of $\hat{C}^T_{xy}/\sqrt{\hat{C}^T_{xx}\hat{C}^T_{yy}}$ tends to its expected value. In order to find a solution for γ, we therefore need to evaluate the integrals of $\hat{C}^T_{xy}/\sqrt{\hat{C}^T_{xx}\hat{C}^T_{yy}}$ over the $\phi^{N,M}$ from 0 to 2π, that is,

$$\gamma = \frac{1}{(2\pi)^{N\times M}}\int_0^{2\pi}\frac{\hat{C}^T_{xy}}{\sqrt{\hat{C}^T_{xx}}\sqrt{\hat{C}^T_{yy}}}\,\mathrm{d}\phi^{N,M}. \tag{25}$$

As it stands, solving these integrals is not a trivial exercise and we therefore resort to perturbation theory: we will rewrite the integrand as a Taylor series in the incoherent terms. Let us therefore first write the cross-correlation and autocorrelations in terms of their coherent and incoherent terms, that is,

$$\frac{\hat{C}^T_{xy}}{\sqrt{\hat{C}^T_{xx}\hat{C}^T_{yy}}} = \frac{\hat{C}_{xyC}+\hat{C}^T_{xyI}}{\sqrt{\hat{C}_{xxC}+\hat{C}^T_{xxI}}\sqrt{\hat{C}_{yyC}+\hat{C}^T_{yyI}}}, \tag{26}$$

Based on empirical arguments (Weemstra *et al.* 2013), we suspect the solution for ρ not an unreasonable proxy for γ and therefore pretend the incoherent terms in the right-hand side of eq. (26) to be small. To that end, we introduce the auxiliary parameter ϵ,

$$\frac{\hat{C}_{xyC}+\hat{C}^T_{xyI}}{\sqrt{\hat{C}_{xxC}+\hat{C}^T_{xxI}}\sqrt{\hat{C}_{yyC}+\hat{C}^T_{yyI}}} \rightarrow \frac{\hat{C}_{xyC}+\epsilon\,\hat{C}^T_{xyI}}{\sqrt{\hat{C}_{xxC}+\epsilon\,\hat{C}^T_{xxI}}\sqrt{\hat{C}_{yyC}+\epsilon\,\hat{C}^T_{yyI}}}. \tag{27}$$

Note that $\epsilon = 0$ implies that the solution for γ coincides with that for ρ.

A Taylor expansion in the small parameter ϵ yields a power series that quantifies the deviation of (26) from the solution for ρ: a so-called perturbation series. The right-hand side of the mapping in (27) we denote γ_ϵ and its Taylor series about $\epsilon = 0$ is given in Appendix B. This Taylor series can be reformulated in terms of ρ multiplied by a power series in ϵ [see eq. (B6)]. The coefficients of this power series are denoted $\gamma_{\epsilon^0}, \gamma_{\epsilon^1}, \gamma_{\epsilon^2}, \ldots$. Coefficients are explicitly computed up to degree two and given by eqs (B7)–(B9), respectively.

Rewriting (26) as a power series in ϵ, that is, a perturbation with respect to the solution for ρ, is simply a vehicle to be able to evaluate the integrals over the random phases $\phi^{N,M}$. We do not actually expect the incoherent terms to be small for individual realizations. That is to say, if we set ϵ to 1, the perturbation associated with the amplitude of the incoherent terms might not be so small. Importantly however, we do anticipate the expected value of the perturbation to be small. With this rationale we therefore set $\epsilon = 1$ in eq. (B6). This implies that we can compute γ by simply calculating the expected value of the coefficients $\gamma_{\epsilon^0}, \gamma_{\epsilon^1}, \gamma_{\epsilon^2}, \ldots$. The independent identically distributed source phases ϕ_{jp} allow us to follow the same procedure as for the earlier calculation of the expected value of the cross-correlation: the expected value of γ_ϵ (with $\epsilon = 1$) is obtained by integrating the coefficients over the phases ϕ_{jp} from 0 to 2π, that is,

$$\gamma = E[\gamma_{\epsilon=1}] = \frac{\rho}{(2\pi)^N}\int_0^{2\pi}\gamma_{\epsilon^0}+\gamma_{\epsilon^1}+\gamma_{\epsilon^2}+\mathcal{O}(\gamma_{\epsilon^3})\,\mathrm{d}\phi^{N,M}. \tag{28}$$

We neglect the expected values of terms that or of order higher than the second degree and denote this approximation γ_{ap}, that is,

$$\gamma_{\mathrm{ap}} = \rho\left(E[\gamma_{\epsilon^0}]+E[\gamma_{\epsilon^1}]+E[\gamma_{\epsilon^2}]\right). \tag{29}$$

The calculation of the expected values of the higher order terms is technically involved and their behaviour is slightly peculiar. Resummations or other techniques might be needed, these issues are currently under investigation. Numerical calculations of γ presented in Section 4 suggest, however, that $E[\gamma_{\epsilon=1}]$ (and hence γ) is sufficiently approximated by γ_{ap}. Actually, we will show later in this section that $E[\gamma_{\epsilon=1}]$ can be approximated even further by approximating the expected value of γ_{ϵ^2}.

The expected values of γ_{ϵ^0}, γ_{ϵ^1} and γ_{ϵ^2} are given by the integrals in eq. (28), and are calculated in Appendix C. The expected value of γ_{ϵ^0} equals 1 and the expected value of γ_{ϵ^1}, given by eq. (C1), equates to zero. The expected value of γ_{ϵ^2} is computed according to eq. (C2) and results in summations over source contributions as is shown in eqs (C3) and (C4). The expected values in eq. (C2) are given by eqs (C5)–(C9). We rewrite the first term in these equations to account for the $k \neq j$ exception of the second sum, that is,

$$\sum_{j=1}^{N}\sum_{k\neq j} f_{jx}f^*_{ky}f_{kx}f^*_{jy} = \sum_{j=1}^{N}\sum_{k=1}^{N} f_{jx}f^*_{ky}f_{kx}f^*_{jy} - \sum_{j=1}^{N} f_{jx}f^*_{jy}f_{jx}f^*_{jy}. \tag{30}$$

Consequently, the second term of each of the eqs (C5)–(C9) reduces in amplitude from $(1-1/M)$ to $1/M$.

The behaviour of γ (and hence γ_{ap}) as a function of distance between $\boldsymbol{x}$ and $\boldsymbol{y}$ is dictated by the distribution of sources and their amplitudes. In order to be able to explicitly solve for specific distributions of sources, we transform the summations over sources into integrations over these sources. The summation over N discrete sources at locations $\boldsymbol{s}_j$ turns into an integral $\int_S \mathrm{d}\boldsymbol{s}$ over surface area $\boldsymbol{s}$. To that end, we transform the discrete f_{jx} into a continuous distribution f_{sx} using the continuous equivalent of the right-hand-side of eq. (7), that is,

$$f_{sx} \equiv \frac{\mathrm{i}}{4}A_s H_0\left(\frac{r_{sx}\omega}{c}\right)\mathrm{e}^{-\alpha r_{sx}}. \tag{31}$$

A_s is the source density as a function of location $\boldsymbol{s}$ and replaces $\hat{S}$ in eq. (7) because we consider a single frequency only; r_{sx} denotes the distance between that location and receiver $\boldsymbol{x}$. Note that A_s includes an implicit normalization dependent on the density of the discrete sources (i.e. a constant with units m^{-2}), which ensures that the evaluation of the integrals and the result of the summations give equal values and have equal units. Using the continuous f_{sx}, the coherent terms, defined in eq. (10), become,

$$\hat{C}_{xyC} = \int_S f_{sx}f^*_{sy}\,\mathrm{d}\boldsymbol{s}, \tag{32}$$

$$\hat{C}_{xxC} = \int_S f_{sx} f_{sx}^* \, \mathrm{d}\boldsymbol{s} \tag{33}$$

and

$$\hat{C}_{yyC} = \int_S f_{sy} f_{sy}^* \, \mathrm{d}\boldsymbol{s}. \tag{34}$$

Interestingly, the double sum in the right-hand side of eq. (30) can be written as the product of two sums, or, equivalently, the product of two integrals. For example, the double sum associated with $E[\hat{C}_{xxI}^{T\,2}]$, that is, eq. (C5), can be written as $\sum_{j=1}^{N} f_{jx} f_{jx}^* \times \sum_{k=1}^{N} f_{kx}^* f_{kx}$. This product translates to $\int_S f_{sx} f_{sx}^* \, \mathrm{d}\boldsymbol{s} \times \int_S f_{s'x}^* f_{s'x} \mathrm{d}\boldsymbol{s}'$ which coincides with $\hat{C}_{xxC}^2$. The expected values of the products of the incoherent terms in γ_{ϵ^2}, that is, eqs (C5)–(C9), therefore translate to the following integrals, respectively,

$$E\left[\hat{C}_{xxI}^{T\,2}\right] = \int_S \int_S f_{sx} f_{s'x}^* f_{s'x} f_{sx}^* \, \mathrm{d}\boldsymbol{s} \, \mathrm{d}\boldsymbol{s}' - \frac{1}{M} \int_S f_{sx}^2 f_{sx}^{*2} \, \mathrm{d}\boldsymbol{s}$$
$$= \hat{C}_{xxC}^2 - \frac{1}{M} \int_S f_{sx}^2 f_{sx}^{*2} \, \mathrm{d}\boldsymbol{s}, \tag{35}$$

$$E\left[\hat{C}_{yyI}^{T\,2}\right] = \int_S \int_S f_{sy} f_{s'y}^* f_{s'y} f_{sy}^* \, \mathrm{d}\boldsymbol{s} \, \mathrm{d}\boldsymbol{s}' - \frac{1}{M} \int_S f_{sy}^2 f_{sy}^{*2} \, \mathrm{d}\boldsymbol{s}$$
$$= \hat{C}_{yyC}^2 - \frac{1}{M} \int_S f_{sy}^2 f_{sy}^{*2} \, \mathrm{d}\boldsymbol{s}, \tag{36}$$

$$E\left[\hat{C}_{xyI}^T \hat{C}_{xxI}^T\right] = \int_S \int_S f_{sx} f_{s'y}^* f_{s'x} f_{sx}^* \, \mathrm{d}\boldsymbol{s} \, \mathrm{d}\boldsymbol{s}' - \frac{1}{M} \int_S f_{sx}^2 f_{sy}^* f_{sx}^* \, \mathrm{d}\boldsymbol{s}$$
$$= \hat{C}_{xxC} \hat{C}_{xyC} - \frac{1}{M} \int_S f_{sx}^2 f_{sy}^* f_{sx}^* \, \mathrm{d}\boldsymbol{s}, \tag{37}$$

$$E\left[\hat{C}_{xyI}^T \hat{C}_{yyI}^T\right] = \int_S \int_S f_{sx} f_{s'y}^* f_{s'y} f_{sy}^* \, \mathrm{d}\boldsymbol{s} \, \mathrm{d}\boldsymbol{s}' - \frac{1}{M} \int_S f_{sy}^{*2} f_{sx} f_{sy} \, \mathrm{d}\boldsymbol{s}$$
$$= \hat{C}_{yyC} \hat{C}_{xyC} - \frac{1}{M} \int_S f_{sy}^{*2} f_{sx} f_{sy} \, \mathrm{d}\boldsymbol{s} \tag{38}$$

and

$$E\left[\hat{C}_{xxI}^T \hat{C}_{yyI}^T\right] = \int_S \int_S f_{sx} f_{s'x}^* f_{s'y} f_{sy}^* \, \mathrm{d}\boldsymbol{s} \, \mathrm{d}\boldsymbol{s}' - \frac{1}{M} \int_S f_{sx} f_{sx}^* f_{sy} f_{sy}^* \, \mathrm{d}\boldsymbol{s}$$
$$= \hat{C}_{xyC} \hat{C}_{yxC} - \frac{1}{M} \int_S f_{sx} f_{sx}^* f_{sy} f_{sy}^* \, \mathrm{d}\boldsymbol{s}. \tag{39}$$

In Appendix D we calculate γ_{ap} for sources distributed uniformly on a ring in the far field. The integrals in eqs (32)–(34) are explicitly solved for such a source distribution in Appendix E. In Appendix F the behaviour of (35)–(39) is explicitly computed. It becomes clear from the expressions obtained in Appendix F that the single integrals of products of four $f_{sx,y}$ in eqs (35)–(39) only add small corrections to the final solution for γ_{ap} (see Appendix D). Moreover, for $M > 1$, the corrections's amplitudes decreases as $1/M$ and hence will be smaller even. Although the corrections are found to be small, specifically assuming sources distributed randomly on a ring in the far field, we believe that that finding can be generalized to any source distribution. This belief stems from the excellent fit we obtain to numerically computed values of γ without accounting for these terms. This comparison is made in Section 4 for two arbitrary source distributions. We will therefore neglect these single integrals in (35)–(39) and hence obtain an approximation of $E\,[\gamma_{\epsilon^2}]$. This approximation is obtained by substituting the coherent terms associated with the double integrals for the expected values in eq. (C2),

$$E\,[\gamma_{\epsilon^2}] \cong \frac{3\hat{C}_{xxC}^2}{8\hat{C}_{xxC}^2} + \frac{3\hat{C}_{yyC}^2}{8\hat{C}_{yyC}^2} - \frac{\hat{C}_{xyC}\hat{C}_{xxC}}{2\hat{C}_{xyC}\hat{C}_{xxC}}$$
$$- \frac{\hat{C}_{xyC}\hat{C}_{yyC}}{2\hat{C}_{xyC}\hat{C}_{yyC}} + \frac{\hat{C}_{xyC}\hat{C}_{yxC}}{4\hat{C}_{xxC}\hat{C}_{yyC}}$$
$$= -\frac{1}{4} + \frac{1}{4}\frac{\hat{C}_{xyC}\hat{C}_{yxC}}{\hat{C}_{xxC}\hat{C}_{yyC}}. \tag{40}$$

Since, by definition, $C_{yxC} = C_{xyC}^*$, we recognize, using eq. (22), that (40) coincides with $-1/4 + (1/4)|\rho|^2$. We introduce the 'coherent approximation', denoted γ_{apC}, which approximates γ_{ap} in the sense that $E\,[\gamma_{\epsilon^2}]$ in (29) is approximated by (40). Note that this approximation is exact in case M tends to infinity. Substituting this approximation and the expected values of γ_{ϵ^0} and γ_{ϵ^1}, that is, 1 and 0, respectively (see Appendix C), in eq. (29), we obtain,

$$\gamma_{\mathrm{apC}} = \frac{3}{4}\rho + \frac{|\rho|^2}{4}\,\rho. \tag{41}$$

It is useful to note that, in case of an isotropic distribution of sources, ρ is purely real (Tsai 2011), which implies that $|\rho|^2 = \rho^2$. We therefore recognize that for such a distribution of sources $\gamma_{\mathrm{apC}} = (3/4)\rho + (1/4)\rho^3$.

We can next use the results of Tsai (2011) who demonstrates how the source distribution governs the behaviour of ρ as a function of inter-receiver distance r_{xy}. The source distribution is described with respect to the point centred between the two receivers at $\boldsymbol{x}$ and $\boldsymbol{y}$. In cases with sufficient sources sufficiently far away, ρ behaves as a decaying oscillating function. For example, for an isotropic distribution of sources, ρ behaves as a decaying Bessel function of order zero, where the decay depends on the subsurface attenuation, that is, α, and the radial distribution of sources. For an anisotropic distribution of sources, in turn, the behaviour of ρ can be described by a series of Bessel functions of order $1 \ldots n$ where the weight of the higher order Bessel functions scales with the degree of anisotropy of the source distribution (see, e.g. also Harmon *et al.* 2010). The bottom line is that for greater receiver separations, the second term on the right-hand side of (41) will tend to zero significantly faster than the first term. Our result therefore suggests that, irrespective of the source distribution, the behaviour of γ is dominated by the first term on the right-hand side of (41) for greater receiver separations.

By computing γ numerically for two arbitrary source distributions, we confirm in Section 4 that, despite our approximations, the behaviour of γ is well described by eq. (41). First, however, we briefly discuss a somewhat surprising result arising from our analysis. We showed in Section 3.1 that averaging the cross-correlation over many different time windows renders the amplitude of the cross-terms negligible, that is, their expected values are zero. As pointed out at the end of Section 2, however, eq. (14) suggests that averaging over very long time, instead of over many different time windows, does not reduce the relative amplitude of the cross-terms. We believe, however, that the fact that the cross-terms of the cross-spectrum do not cancel for large T does not imply that the cross-terms of the cross-correlation do not cancel for large T. In fact, we suspect that this cancellation is inherent in the computation of the inverse Fourier transform. Although it will not be proven explicitly here, qualitatively it can be understood by considering (i) the leakage to adjacent frequencies associated with the finite

realization time T_a and (ii) the sampling in the frequency domain due to the length of the chosen cross-correlation window T.

The leakage due to the finite realization time results in a squared sinc function in the cross-spectrum, that is, $\mathrm{sinc}^2\left[(\omega_0 - \omega)\, T_a/2\right]$. The peak of this function has an approximate width of $\Delta^{\omega}_{T_a} \equiv 2\pi/T_a$. In practice, DFTs are often computed in order to calculate the cross-correlation: the spectrum at x is multiplied by the complex conjugate of the spectrum at y after which the cross-correlation is obtained through computation of the inverse DFT of the cross-spectrum. The DFT associated with a cross-correlation window of length $T \gg T_A$ has a sampling interval in the frequency domain of $\Delta^{\omega}_{T} \equiv 2\pi/T$. Expressing $\Delta^{\omega}_{T_a}$ in terms of T and T_a, we have, $\Delta^{\omega}_{T_a} = M\Delta^{\omega}_{T}$. Computation of the inverse DFT of $\hat{C}^{T}_{xy}$ over a bandwidth $\Delta^{\omega}_{T_a}$ may well cause cross-terms to become vanishingly small in the time domain. Similarly, we expect the cross-terms of the autocorrelation to stack incoherently in case an M-point smoothed spectral density function is computed (i.e. conform Lawrence & Prieto 2011). A formal derivation, however, is beyond the scope of this work.

4 NUMERICAL VERIFICATION

For two arbitrary source distributions we calculate ρ and γ numerically, using eqs (17) and (23), respectively. We assume $T = T_a$ (M = 1) and hence the cross-spectrum is given by eq. (8), that is, $\hat{C}^{T}_{xy} = \hat{C}_{xy}$, which implies that the coherent and incoherent terms are given by eqs (10) and (11), respectively. The phase velocity c is assumed spatially invariant and, since our model is monochromatic, we prescribe the geometry in terms of the wavelength considered. Cross-spectra are calculated for pairs of receivers equidistant from the centre of the distribution of sources (see Fig. 1). Inter-receiver distances are incremented by $\lambda/30$, starting at $r_{xy} = 0$. For each receiver, we simply compute eq. (4) with source contributions computed using the exact Green's function given by eq. (3). These sources are given random phases between 0 and 2π.

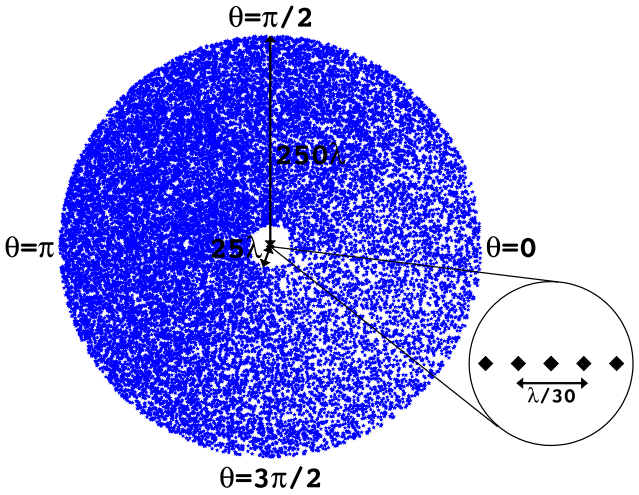

Figure 1. The setup of the numerical experiment. Sources, in blue, are randomly placed [with the probability defined by (42) in this case] on a circle with outer radius 250λ and inner radius 25λ. The bottom right zooms in on the very centre of the experiment and shows a blow-up of the line of receivers. The receiver separation increments with λ/30.

A total of two-and-a-half million sources ($N = 2.5 \times 10^6$) are randomly placed with the probability prescribed by the source density function $A_s(\theta, r)$, which in a first experiment we define,

$$A_s(\theta, r) = \begin{cases} \frac{3}{4} + \frac{1}{4}\cos(\theta - \frac{5\pi}{6}), & 25\lambda < r < 250\lambda \\ 0, & \text{otherwise,} \end{cases} \tag{42}$$

and in the following experiment we define,

$$A_s(\theta, r) = \begin{cases} \frac{1}{2} + \frac{1}{2}\cos(2\theta), & 25\lambda < r < 250\lambda \\ 0, & \text{otherwise.} \end{cases} \tag{43}$$

We subsequently calculate the autocorrelations and cross-correlations, that is, we compute expression (8). Averaging over a total of 25 000 realizations ($W = 2.5 \times 10^4$), where source phases change randomly between realizations, we then calculate ρ and γ using eqs (17) and (23), respectively. Note that we do not average over the azimuth (and hence do not compute $\bar{\rho}$ and $\bar{\gamma}$), because all our receivers are placed along a single line.

Fig. 2 shows the results for both experiments for a prescribed attenuation of $\alpha = 0.15/\lambda$. Both the real (circles) and imaginary (triangles) parts of ρ (blue) and γ (green) are plotted. The black curves are calculated by substituting the obtained values for ρ in eq. (41). Despite our approximations, we observe that γ_{apC} coincides well with the behaviour of the numerically computed γ values for both source distributions. The red curve gives the behaviour solely due to the first term at the right-hand side of this equation, that is, three quarters of ρ. For greater distances, the behaviour of the numerically computed γ values is well explained by this term only. The high amplitudes of the real part in **b** can be explained by the relatively high number of sources in the stationary-phase directions in the second experiment, that is, source density function (43). Fig. 3 exemplifies the distribution of individual $\hat{C}_{xy}/\sqrt{\langle \hat{C}_{xx}\rangle\langle \hat{C}_{yy}\rangle}$ and individual $\hat{C}_{xy}/|\hat{C}_{xy}|$ for a station separation of $\sim$1.6λ. It illustrates how the collapse of individual $\hat{C}_{xy}$ on the unit circle results in an amplitude decrease of $\sim$25 per cent.

5 DISCUSSION AND CONCLUSIONS

The theoretical framework provided by Tsai (2011) illustrates how the whitened averaged coherency behaves as a function of inter-receiver distance for different source distributions. Most notably, he derives how its decay, and hence that of its azimuthal average, varies as a function of source distribution in the presence of attenuation. His results are very useful, but, in order to make proper use of them, one needs to make sure that the whitened averaged coherency is properly obtained from the data. That is to say, the data processing needs to be adequate in the sense that the cross-terms (i.e. the incoherent parts in our model) cancel out and expression (22) is effectively implemented. This is, in practice, not a trivial task, especially since the (average) source correlation time is unknown. The length of the interval over which the ambient seismic field needs to be averaged to make the cross-terms cancel out is therefore unknown.

There are two additional issues that make it difficult to retrieve the whitened averaged coherency as defined by eq. (22) from ambient seismic noise data. First, time-series are frequently interrupted by transient large-amplitude pulses, for example, earthquake signals. Second, the ambient seismic field is essentially non-stationary, also at the frequencies dominated by microseismic signal. It might be stationary over shorter intervals, ranging from a few hours to a few

days, but over timespans of months to years, which generally are the periods for which data are collected in interferometric surface wave studies, it is rather non-stationary. This has been recognized by researchers in the SPAC community before (see e.g. Okada 2003). The rate at which the power of the ambient seismic field fluctuates may even be higher than the time needed for cross-terms to cancel out. It is, for that reason, rather useful that normalization and cancellation can be reversed. The newly derived approximation, that is, expression (41), accounts for the amplitude decrease associated with this reversal.

An alternative normalization procedure may provide a satisfactory solution to the above-mentioned difficulties in retrieving the whitened averaged coherency. As noted previously, substituting the smoothed spectral density functions for the actual spectral density functions in the normalization, may yield fairly correct estimates of the whitened averaged coherency; for example, conform Prieto *et al.* (2009) and Lawrence & Prieto (2011). Of course, the width of the employed frequency band is a parameter that needs to be determined carefully in such case. The relation between this bandwidth, the cancellation of cross-terms, the length of the employed cross-correlation windows and the source correlation time will be a topic of future work.

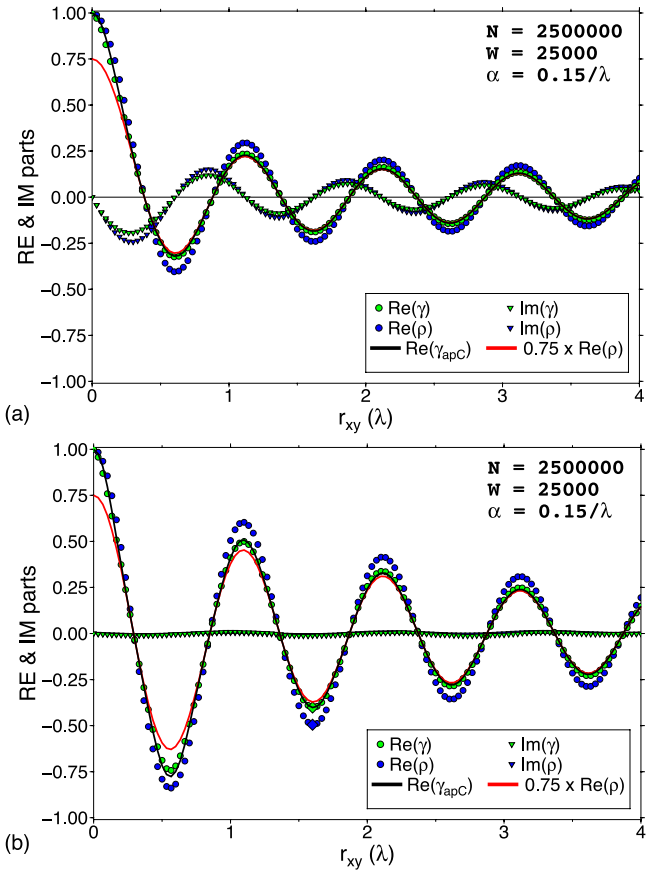

Figure 2. Behaviour of the whitened averaged coherency and the averaged whitened coherency for an attenuating medium with $\alpha = 0.15/\lambda$. We have assumed a coinciding realization time and measurement time, that is, $T/T_a = 1$. The result of the first experiment, with the source distribution prescribed by eq. (42), and shown in Fig. 1, is shown in (a) and that of the second experiment, with the source distribution prescribed by eq. (43), in (b). The green dots and triangles present the real and imaginary parts of the averaged whitened coherency, respectively, as obtained from our numerical experiment. Similarly, the blue dots and triangles present the real and imaginary parts of the whitened averaged coherency, respectively. The black lines depict the behaviour of our analytical approximation of the averaged whitened coherency, that is, eq. (41). The red curves show the behaviour of our approximation in case the second term on the right-hand side of eq. (41) is neglected. For inter-receiver distances larger than approximately two wavelengths, the averaged whitened coherency is approximated correctly by three quarters of the whitened averaged coherency. Distributions of normalized cross-spectra for individual realizations are given in Fig. 3 for the station separation for which Re[ρ] and Re[γ] are depicted by diamonds.

Our result enables us to reinterpret earlier results by Weemstra *et al.* (2013). The procedure adopted by these researchers involved neither averaging of power spectral densities over different cross-correlation windows nor averaging over different discrete frequencies. Their procedure therefore did not allow cross-terms to cancel prior to normalization, which may very well explain the fact that they require the real part of their azimuthally averaged spectrally whitened cross-correlations to be fit by a downscaled, decaying Bessel function, that is, as in eq. (24). They find that the proportionality constant generally varies smoothly with frequency and has values between 0.4 and 0.75. The fact that values below 3/4 are found can be explained by (i) local, non-propagating noise (e.g. instrument noise) and/or (ii) strong (earthquake) events present in the recordings. The fact that we employ a 2-D model in this study, is another potential reason why proportionality constants below 0.75 are required. That is, our model does not take into account possible ambient body wave energy.

Our approximation for the behaviour of the averaged whitened coherency indicates that fitting a downscaled, decaying Bessel function, that is, as in eq. (24), will only result in significant error on the attenuation estimate at relatively small inter-receiver distance. Since surface waves in Weemstra *et al.* (2013) are retrieved from cross-correlations of ambient vibrations recorded over a reservoir, offshore Norway, the aperture of the array of ocean-bottom seismometers is only about 12 km. For frequencies increasing from 0.20 to 0.25 Hz, they find that phase velocities decrease from 1200 to 800 m s^{-1}. This allows for the computation of the azimuthally averaged spectrally whitened cross-correlations up to a maximum of $\sim 2\lambda$ and $\sim 4\lambda$ for surface wave frequencies of 0.20 and 0.25 Hz, respectively. Weemstra *et al.* (2013) find surface wave quality factors increasing from 8 at 0.20 Hz to 15 at 0.25 Hz. They attribute these (relatively) low-quality factors to the local geology. Since the spectrally whitened cross-correlations computed by these researchers should be interpreted as the averaged whitened coherency, instead of the whitened averaged coherency, the employed model was incorrect. In retrospect, a downscaled decaying Bessel function should not have been fitted to the obtained values of at such short inter-receiver distances (with respect to the wavelengths).

Quality factor estimates for pressure-component recordings, reported in the same study, have reasonable values for frequencies between 1.5 and 2.2 Hz. Since phase velocities vary around 2 km s^{-1} for those frequencies, however, up to $\sim$10 wavelengths are sampled by the array of ocean-bottom seismometers. The attenuation coefficient estimates are therefore, contrary to the estimates at $\sim$0.20 Hz, barely biased by the strong decay of azimuthally averaged averaged whitened coherency over the first wavelengths.

In recent years, spectrally whitened cross-spectra associated with single receiver pairs have been used successfully to determine dispersion curves (Ekström *et al.* 2009; Tsai & Moschetti 2010; Boschi *et al.* 2013). The method is based on Aki's derivation for the whitened averaged coherency (Aki 1957). The zeros of the real part of the time-averaged and whitened cross-spectrum are associated with the zeros of a Bessel function to obtain estimates of phase velocity at discrete frequencies. From our derivation it

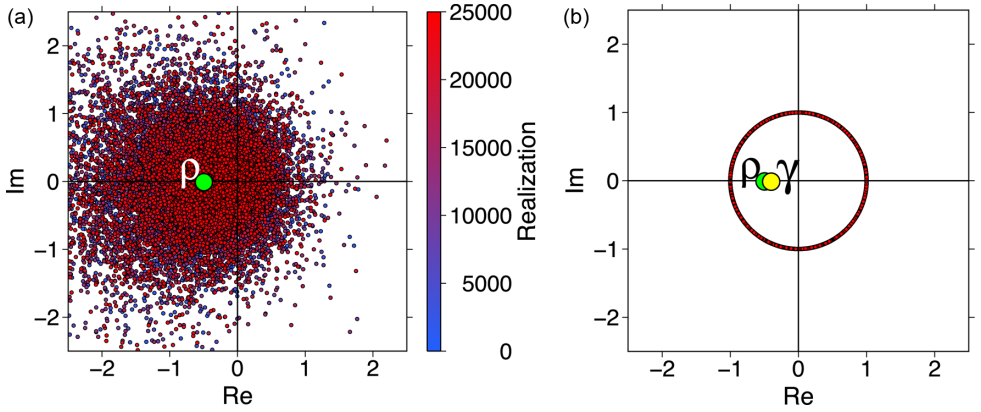

Figure 3. Individual $\hat{C}_{xy}/\sqrt{\langle\hat{C}_{xx}\rangle\langle\hat{C}_{yy}\rangle}$ (a) and individual $\hat{C}_{xy}/|\hat{C}_{xy}|$ (b) for a station separation of ∼1.6λ (see Fig. 2). The geometric mean of the values, that is, ρ in (a) and γ in (b), are shown by a green and yellow dot, respectively. For comparison ρ is also depicted in (b).

follows explicitly that the zero crossings remain unchanged in case cross-terms did not cancel prior to spectral whitening.

Many factors complicate the behaviour of the complex coherency, which recently has been used to estimate subsurface attenuation (Prieto *et al.* 2009; Weemstra *et al.* 2013). Especially the illumination pattern has a significant impact (Tsai 2011). Irrespective of such factors, however, our derivation shows that explicit averaging of the power spectral densities involved in the normalization process is required in order to correctly retrieve the complex coherency. Importantly, if cross-terms do not cancel prior to spectral whitening, our analysis reveals that the retrieved coherency is proportional to the complex coherency at inter-receiver distances larger than two wavelengths. At shorter distances, however, the presence of cross-terms in the normalization process causes the coherency to decay more rapidly. This decay could erroneously be interpreted as subsurface attenuation.

ACKNOWLEDGEMENTS

We gratefully acknowledge support from the QUEST Initial Training Network funded within the EU Marie Curie actions programme. We warmly thank Victor Tsai and Michael Ritzwoller for their careful reading and help in improving the manuscript. LB thanks Domenico Giardini for his constant support and encouragement. This study benefitted from interactions with Stefan Hiemer, Yaver Kamer and Stefano Marano. We owe gratitude to Kuan Li for his patient help with difficult mathematical constructs. Finally, we would like to thank Max Rietmann and Dave May for advising us on parallel computing. Part of the figures were generated with the help of Generic Mapping Tools (Wessel & Smith 1991).

REFERENCES

Abramowitz, M. & Stegun, I.A., 1964. *Handbook of Mathematical Functions with Formulas, Graphs, and Mathematical Tables,* National Bureau of Standards Applied Mathematics Series.

Aki, K., 1957. Space and time spectra of stationary stochastic waves, with special reference to microtremors, *Bull. Earthq. Res. Inst. Univ. Tokyo,* **35,** 415–457.

Arfken, G.B. & Weber, H.J., 2005. *Mathematical Methods for Physicists,* 6th edn, Elsevier Academic Press.

Asten, M.W., 2006. On bias and noise in passive seismic data from finite circular array data processed using SPAC methods, *Geophysics,* **71**(6), V153–V162.

Bensen, G.D., Ritzwoller, M.H., Barmin, M.P., Levshin, A.L., Lin, F., Moschetti, M.P., Shapiro, N.M. & Yang, Y., 2007. Processing seismic ambient noise data to obtain reliable broad-band surface wave dispersion measurements, *Geophys. J. Int.,* **169**(3), 1239–1260.

Boschi, L., Weemstra, C., Verbeke, J., Ekstrom, G., Zunino, A. & Giardini, D., 2013. On measuring surface wave phase velocity from station-station cross-correlation of ambient signal, *Geophys. J. Int.,* **192**(1), 346–358.

Brenguier, F., Shapiro, N.M., Campillo, M., Nercessian, A. & Ferrazzini, V., 2007. 3-D surface wave tomography of the Piton de la Fournaise volcano using seismic noise correlations, *Geophys. Res. Lett.,* **34**(2), L02305, doi:10.1029/2006GL028586.

Bussat, S. & Kugler, S., 2009. Recording noise: estimating shear-wave velocities: feasibility of offshore ambient-noise surface-wave tomography (ANSWT) on a reservoir scale, *SEG Tech. Prog. Exp. Abstr.,* **28**(1), 1627–1631.

Campillo, M. & Paul, A., 2003. Long-range correlations in the diffuse seismic coda, *Science,* **299**(5606), 547–549.

Chávez-García, F.J., Rodríguez, M. & Stephenson, W.R., 2005. An alternative approach to the SPAC analysis of microtremors: exploiting stationarity of noise, *Bull. seism. Soc. Am.,* **95**(1), 277–293.

Claerbout, J.F., 1968. Synthesis of a layered medium from its acoustic transmission response, *Geophysics,* **33**(2), 264–269.

Draganov, D., Campman, X., Thorbecke, J., Verdel, A. & Wapenaar, K., 2009. Reflection images from ambient seismic noise, *Geophysics,* **74**(5), A63–A67.

Draganov, D., Wapenaar, K., Mulder, W., Singer, J. & Verdel, A., 2007. Retrieval of reflections from seismic background-noise measurements, *Geophys. Res. Lett.,* **34**(4), L04305, doi:10.1029/2006GL028735.

Duvall, T.L., Jefferies, S.M., Harvey, J.W. & Pomerantz, M.A., 1993. Time-distance helioseismology, *Nature,* **362**(6419), 430–432.

Ekström, G., Abers, G. & Webb, S., 2009. Determination of surface-wave phase velocities across USArray from noise and Aki's spectral formulation, *Geophys. Res. Lett.,* **36,** L18301, doi:10.1029/2009GL039131.

Hanasoge, S.M., 2013. The influence of noise sources on cross-correlation amplitudes, *Geophys. J. Int.,* **192**(1), 295–309.

Haney, M.M., 2009. Infrasonic ambient noise interferometry from correlations of microbaroms, *Geophys. Res. Lett.,* **36**(19), doi:10.1029/2009GL040179.

Harmon, N., Rychert, C. & Gerstoft, P., 2010. Distribution of noise sources for seismic interferometry, *Geophys. J. Int.,* **183**(3), 1470–1484.

Kohler, M.D., Heaton, T.H. & Bradford, S.C., 2007. Propagating waves in the steel, moment-frame factor building recorded during earthquakes, *Bull. seism. Soc. Am.,* **97**(4), 1334–1345.

Larose, E., Derode, A., Campillo, M. & Fink, M., 2004. Imaging from one-bit correlations of wideband diffuse wave fields, *J. appl. Phys.,* **95**(12), 8393–8399.

Lawrence, J.F. & Prieto, G.A., 2011. Attenuation tomography of the western United States from ambient seismic noise, *J. geophys. Res.,* **116**(B6), B06302, doi:10.1029/2010JB007836.

Lin, F.-C., Tsai, V.C., Schmandt, B., Duputel, Z. & Zhan, Z., 2013. Extracting seismic core phases with array interferometry, *Geophys. Res. Lett.,* **40**(6), 1049–1053.

McNamara, D.E. & Buland, R.P., 2004. Ambient noise levels in the continental United States, *Bull. seism. Soc. Am.,* **94**(4), 1517–1527.

Nakahara, H., 2012. Formulation of the spatial autocorrelation (SPAC) method in dissipative media, *Geophys. J. Int.,* **190**(3), 1777–1783.

Nakata, N., Snieder, R., Tsuji, T., Larner, K. & Matsuoka, T., 2011. Shear wave imaging from traffic noise using seismic interferometry by cross-coherence, *Geophysics,* **76**(6), SA97–SA106.

Okada, H., 2003. *The Microtremor Survey Method,* Geophysical Monograph, No. 12, Society of Exploration Geophysicists.

Olofsson, B., 2010. Marine ambient seismic noise in the frequency range 1–10 Hz, *Leading Edge,* **29**(4), 418–435.

Peter, D., Tape, C., Boschi, L. & Woodhouse, J.H., 2007. Surface wave tomography: global membrane waves and adjoint methods, *Geophys. J. Int.,* **171**(3), 1098–1117.

Peterson, J., 1993. Observation and modeling of seismic background noise. Open-File Rep, *U.S. Geol. Surv., 93-322*.

Poli, P., Pedersen, H.A., Campillo, M. & the POLENET/LAPNET Working Group, 2012. Emergence of body waves from cross-correlation of short period seismic noise, *Geophys. J. Int.,* **188**(2), 549–558.

Prieto, G.A., Lawrence, J.F. & Beroza, G.C., 2009. Anelastic Earth structure from the coherency of the ambient seismic field, *J. geophys. Res.,* **114,** B07303, doi:10.1029/2008JB006067.

Rickett, J. & Claerbout, J., 1999. Acoustic daylight imaging via spectral factorization: helioseismology and reservoir monitoring, *Leading Edge,* **18**(8), 957–960.

Ringler, A.T. & Hutt, C.R., 2010. Self-noise models of seismic instruments, *Seism. Res. Lett.,* **81**(6), 972–983.

Roux, P. & Fink, M., 2003. Green's function estimation using secondary sources in a shallow water environment, *J. acoust. Soc. Am.,* **113**(3), 1406–1416.

Sabra, K., Gerstoft, P., Roux, P., Kuperman, W. & Fehler, M., 2005. Extracting time-domain Green's function estimates from ambient seismic noise, *Geophys. Res. Lett.,* **32,** L03310, doi:10.1029/2004GL021862.

Seats, K.J., Lawrence, J.F. & Prieto, G.A., 2012. Improved ambient noise correlation functions using Welch's method, *Geophys. J. Int.,* **188**(2), 513–523.

Shapiro, N.M. & Campillo, M., 2004. Emergence of broadband Rayleigh waves from correlations of the ambient seismic noise, *Geophys. Res. Lett.,* **31**(7), L07614, doi:10.1029/2004GL019491.

Shapiro, N.M., Campillo, M., Stehly, L. & Ritzwoller, M.H., 2005. High-resolution surface-wave tomography from ambient seismic noise, *Science,* **307**(5715), 1615–1618.

Sleeman, R., van Wettum, A. & Trampert, J., 2006. Three-channel correlation analysis: a new technique to measure instrumental noise of digitizers and seismic sensors, *Bull. seism. Soc. Am.,* **96**(1), 258–271.

Snieder, R., 2004. Extracting the Green's function from the correlation of coda waves: a derivation based on stationary phase, *Phys. Rev. E,* **69**(4), doi:10.1103/PhysRevE.69.046610.

Snieder, R. & Åžafak, E., 2006. Extracting the building response using seismic interferometry: theory and application to the Millikan Library in Pasadena, California, *Bull. seism. Soc. Am.,* **96**(2), 586–598.

Tsai, V.C., 2011. Understanding the amplitudes of noise correlation measurements, *J. geophys. Res.,* **116**(B9), B09311, doi:10.1029/2011JB008483.

Tsai, V.C. & Moschetti, M.P., 2010. An explicit relationship between time-domain noise correlation and spatial autocorrelation (SPAC) results, *Geophys. J. Int.,* **182**(1), 454–460.

Verbeke, J., Boschi, L., Stehly, L., Kissling, E. & Michelini, A., 2012. High-resolution Rayleigh-wave velocity maps of central Europe from a dense ambient-noise data set, *Geophys. J. Int.,* **188**(3), 1173–1187.

Wapenaar, C., Draganav, D., Snieder, R., Campman, X. & Verdel, A., 2010. Tutorial on seismic interferometry: part 1—basic principles and applications, *Geophysics,* **75**(5), 75A195–75A209.

Wapenaar, K., van der Neut, J., Ruigrok, E., Draganov, D., Hunziker, J., Slob, E., Thorbecke, J. & Snieder, R., 2011. Seismic interferometry by crosscorrelation and by multidimensional deconvolution: a systematic comparison, *Geophys. J. Int.,* **185**(3), 1335–1364.

Weaver, R.L., 2012. On the retrieval of attenuation from the azimuthally averaged coherency of a diffuse field, preprint, arXiv:1206.6513.

Weaver, R.L. & Lobkis, O.I., 2001. Ultrasonics without a source: thermal fluctuation correlations at MHz Frequencies, *Phys. Rev. Lett.,* **87**(13), 134301, doi:10.1103/PhysRevLett.87.134301.

Weaver, R. & Lobkis, O., 2002. On the emergence of the Green's function in the correlations of a diffuse field: pulse-echo using thermal phonons, *Ultrasonics,* **40**(1-8), 435–439.

Weemstra, C., Boschi, L., Goertz, A. & Artman, B., 2013. Seismic attenuation from recordings of ambient noise, *Geophysics,* **78**(1), Q1–Q14.

Wessel, P. & Smith, W., 1991. Free software helps map and display data, *EOS Trans.,* **72,** 441–446.

Yang, Y., Ritzwoller, M.H., Levshin, A.L. & Shapiro, N.M., 2007. Ambient noise Rayleigh wave tomography across Europe, *Geophys. J. Int.,* **168**(1), 259–274.

Yokoi, T. & Margaryan, S., 2008. Consistency of the spatial autocorrelation method with seismic interferometry and its consequence, *Geophys. Prospect.,* **56**(3), 435–451.

APPENDIX A: FOURIER TRANSFORM OF A SOURCE'S SIGNAL

We define the Fourier transform of a real function $g(t)$ as

$$\hat{g}(\omega) \equiv \frac{1}{\sqrt{2\pi}} \int_{-\infty}^{\infty} g(t) \mathrm{e}^{-\mathrm{i}\omega t} \mathrm{d}t. \tag{A1}$$

Consider a time-limited cosine oscillating with an angular frequency of ω_0 and with arbitrary phase ϕ over a period of T_a seconds, that is

$$u(t) \equiv \begin{cases} 0, & t < -T_a/2 \\ A\cos(\omega_0 t + \phi), & -T_a/2 \leq t \leq T_a/2 \\ 0, & t > T_a/2, \end{cases} \tag{A2}$$

where A denotes the amplitude of the cosine. The Fourier transform of this function is obtained by convolving the Fourier transform of a boxcar with that of an infinite cosine oscillating with the same frequency ω_0. The Fourier transform of a unit amplitude boxcar with width T_a and centred around $t = 0$ is given by $(T_a/\sqrt{2\pi})\mathrm{sinc}(\omega T_a/2)$. The Fourier transform of a cosine function oscillating with an angular frequency ω_0, phase shift ϕ and amplitude A is given by $(A\pi/\sqrt{2\pi})[\delta(\omega_0 - \omega)\mathrm{e}^{\mathrm{i}\phi} + \delta(\omega_0 + \omega)\mathrm{e}^{-\mathrm{i}\phi}]$. Convolving the two results and ignoring the negative frequency contribution, because we are dealing with real functions only, yields

$$\hat{u}(\omega, T_a) = \frac{A T_a \ \mathrm{sinc}[(\omega_0 - \omega)\, T_a/2]}{2\sqrt{2\pi}} \mathrm{e}^{\mathrm{i}\phi}. \tag{A3}$$

Note that the convolution includes multiplication by a factor $1/\sqrt{2\pi}$ due to the normalization convention of the Fourier transform adopted in eq. (A1). The sinc function formalizes the leakage to frequencies adjacent to ω_0, which is due to the finite nature of the time window. This leakage decreases as T_a increases.

Let us now consider a sequence of M cosines oscillating with the same angular frequency ω_0 and constant amplitude A, but with different random phases ϕ_j. With this sequence starting at $t = 0$ we have:

$$u_T(t) \equiv \begin{cases} A\cos(\omega_0 t + \phi_1), & 0 \le t < T_a \\ \vdots & \vdots \\ A\cos(\omega_0 t + \phi_j), & (j-1)T_a \le t < jT_a \\ \vdots & \vdots \\ A\cos(\omega_0 t + \phi_M), & (M-1)T_a \le t < MT_a. \end{cases} \tag{A4}$$

The Fourier transform of this sequence is hence computed by

$$\hat{u}_T(\omega, T_a) = \frac{A}{\sqrt{2\pi}} \sum_{j=1}^{M} \int_{(j-1)T_a}^{jT_a} \cos(\omega_0 t + \phi_j)\, \mathrm{e}^{-\mathrm{i}\omega t}\, \mathrm{d}t. \tag{A5}$$

By changing the integration variable $t = t' + jT_a - T_a/2$ for each element of the sum, the integrals in eq. (A5) can be evaluated using our result in eq. (A3). The Fourier transform of the boxcar experiences a phase shift of $(\omega - \omega_0)(jT_a - T_a/2)$ due to the change of integration variable. This phase shift accounts for the change in starting time ($t = 0$ instead of $t = T_a/2$) and the forward stepping in time with steps jT_a. Again only considering the positive frequencies, we find,

$$\hat{u}_T(\omega, T_a) = \frac{AT_a\ \mathrm{sinc}[(\omega_0 - \omega)\, T_a/2]}{2\sqrt{2\pi}} \sum_{j=1}^{M} \mathrm{e}^{\mathrm{i}\phi_j}\, \mathrm{e}^{\mathrm{i}(\omega_0-\omega)(jT_a - T_a/2)}. \tag{A6}$$

APPENDIX B: SERIES APPROXIMATION FOR γ

The Taylor expansion about $\epsilon = 0$ is given by,

$$\begin{aligned} \gamma_\epsilon &\equiv \frac{\hat{C}_{xyC} + \epsilon\, \hat{C}^T_{xyI}}{\sqrt{\hat{C}_{xxC} + \epsilon\, \hat{C}^T_{xxI}}\sqrt{\hat{C}_{yyC} + \epsilon\, \hat{C}^T_{yyI}}} \\ &= \gamma_\epsilon^{(0)}(\epsilon = 0) + \gamma_\epsilon^{(1)}(\epsilon = 0)\, \epsilon + \frac{\gamma_\epsilon^{(2)}(\epsilon = 0)}{2!}\, \epsilon^2 + \ldots + \frac{\gamma_\epsilon^{(n)}(\epsilon = 0)}{n!}\, \epsilon^n + \ldots, \end{aligned} \tag{B1}$$

where $\gamma_\epsilon^{(n)}$ denotes the n-th derivative of γ_ϵ and $n!$ the factorial of n.

We calculate the derivatives of γ_ϵ up to the second order and substitute $\epsilon = 0$ to obtain,

$$\gamma_\epsilon^{(0)}(0) = \frac{\hat{C}_{xyC}}{\sqrt{\hat{C}_{xxC}\hat{C}_{yyC}}}, \tag{B2}$$

$$\gamma_\epsilon^{(1)}(0) = \frac{\hat{C}^T_{xyI}}{\sqrt{\hat{C}_{xxC}\hat{C}_{yyC}}} - \frac{\hat{C}_{xyC}\left(\hat{C}^T_{xxI}\hat{C}_{yyC} + \hat{C}_{xxC}\hat{C}^T_{yyI}\right)}{2\hat{C}_{xxC}\hat{C}_{yyC}\sqrt{\hat{C}_{xxC}\hat{C}_{yyC}}}, \tag{B3}$$

and

$$\gamma_\epsilon^{(2)}(0) = \frac{3\hat{C}^{T\,2}_{xxI}\hat{C}_{xyC}\hat{C}^2_{yyC} - 4\hat{C}_{xxC}\hat{C}^T_{xxI}\hat{C}^T_{xyI}\hat{C}^2_{yyC}}{4\hat{C}^2_{xxC}\hat{C}^2_{yyC}\sqrt{\hat{C}_{xxC}\hat{C}_{yyC}}} + \frac{2\hat{C}_{xxC}\hat{C}^T_{xxI}\hat{C}_{xyC}\hat{C}_{yyC}\hat{C}^T_{yyI} - 4\hat{C}^2_{xxC}\hat{C}^T_{xyI}\hat{C}_{yyC}\hat{C}^T_{yyI} + 3\hat{C}^2_{xxC}\hat{C}_{xyC}\hat{C}^{T\,2}_{yyI}}{4\hat{C}^2_{xxC}\hat{C}^2_{yyC}\sqrt{\hat{C}_{xxC}\hat{C}_{yyC}}}, \tag{B4}$$

respectively.

We recognize that ρ can be extracted from the expressions $\gamma_\epsilon^{(n)}(0)$ and account for the division by the factorials, defining

$$\gamma_{\epsilon^n} \equiv \frac{1}{n!}\frac{\gamma_\epsilon^{(n)}(0)}{\rho}. \tag{B5}$$

Substituting these expressions in the series in eq. (B1), this series is written as a power series in ϵ multiplied by ρ, that is,

$$\gamma_\epsilon = \rho\left[\gamma_{\epsilon^0} + \gamma_{\epsilon^1}\epsilon + \gamma_{\epsilon^2}\epsilon^2 + \mathcal{O}\left(\epsilon^3\right)\right]. \tag{B6}$$

Substituting expressions (B2)–(B4) in eq. (B5), we obtain the coefficients γ_{ϵ^0}, γ_{ϵ^1} and γ_{ϵ^2}, respectively. We find:

$$\gamma_{\epsilon^0} = 1, \tag{B7}$$

$$\gamma_{\epsilon^1} = \frac{\hat{C}^T_{xyI}}{\hat{C}_{xyC}} - \frac{\hat{C}^T_{xxI}}{2\hat{C}_{xxC}} - \frac{\hat{C}^T_{yyI}}{2\hat{C}_{yyC}} \tag{B8}$$

and

$$\gamma_{\epsilon^2} = \frac{3\hat{C}^{T\ 2}_{xxI}}{8\hat{C}^2_{xxC}} + \frac{3\hat{C}^{T\ 2}_{yyI}}{8\hat{C}^2_{yyC}} - \frac{\hat{C}^T_{xyI}\hat{C}^T_{xxI}}{2\hat{C}_{xyC}\hat{C}_{xxC}} - \frac{\hat{C}^T_{xyI}\hat{C}^T_{yyI}}{2\hat{C}_{xyC}\hat{C}_{yyC}} + \frac{\hat{C}^T_{xxI}\hat{C}^T_{yyI}}{4\hat{C}_{xxC}\hat{C}_{yyC}}. \tag{B9}$$

APPENDIX C: COMPUTATION OF THE EXPECTED VALUES

We calculate the expected values of γ_{ϵ^0}, γ_{ϵ^1} and γ_{ϵ^2} which are given by eqs (B7)–(B9), respectively. The zeroth-order coefficient γ_{ϵ^0} is equal to 1 and hence $E[\gamma_{\epsilon^0}] = 1$. The expected value of γ_{ϵ^1} is the sum of the expected values of the three terms in eq. (B8). Because the individual elements of the summations associated with these three terms traverse a circle in the complex plane from 0 to 2π, we get [similar to integrands in eq. (21)]

$$\begin{aligned} E[\gamma_{\epsilon^1}] &= \frac{1}{(2\pi)^{N\times M}} \int_0^{2\pi} \frac{\hat{C}^T_{xyI}}{\hat{C}_{xyC}} - \frac{\hat{C}^T_{xxI}}{2\hat{C}_{xxC}} - \frac{\hat{C}^T_{yyI}}{2\hat{C}_{yyC}}\ \mathrm{d}\phi^{N,M} \\ &= 0. \end{aligned} \tag{C1}$$

Similar to the expected value of γ_{ϵ^1}, the expected value of γ_{ϵ^2} is obtained by summing the expected values of the individual terms in eq. (B9). While the denominators consist of products of coherent terms, they are independent of the ϕ_{jp} and hence can be excluded from the expected value computation, that is,

$$\begin{aligned} E[\gamma_{\epsilon^2}] = {} & \frac{3}{8\hat{C}^2_{xxC}} E\left[\hat{C}^{T\ 2}_{xxI}\right] + \frac{3}{8\hat{C}^2_{yyC}} E\left[\hat{C}^{T\ 2}_{yyI}\right] - \frac{1}{2\hat{C}_{xyC}\hat{C}_{xxC}} E\left[\hat{C}^T_{xyI}\hat{C}^T_{xxI}\right] \\ & - \frac{1}{2\hat{C}_{xyC}\hat{C}_{yyC}} E\left[\hat{C}^T_{xyI}\hat{C}^T_{yyI}\right] + \frac{1}{4\hat{C}_{xxC}\hat{C}_{yyC}} E\left[\hat{C}^T_{xxI}\hat{C}^T_{yyI}\right]. \end{aligned} \tag{C2}$$

In general, the expected value of the product of two incoherent terms can be computed by

$$\begin{aligned} E\left[\hat{C}^{T\ 2}_{xyI}\right] = {} & \frac{1}{(2\pi)^{N\times M}} \int_0^{2\pi} \hat{C}^{T\ 2}_{xyI}(\phi^{N,M})\ \mathrm{d}\phi^{N,M} \\ = {} & \frac{1}{(2\pi)^{N\times M} \times M^2} \int_0^{2\pi} \sum_{p=1}^{M}\sum_{q\neq p}^{M}\sum_{r=1}^{M}\sum_{s\neq r}^{M}\sum_{j=1}^{N}\sum_{k=1}^{N} f_{jx} f^*_{jy} f_{kx} f^*_{ky} h_p h^*_q h_r h^*_s \mathrm{e}^{\mathrm{i}(\phi_{jp}-\phi_{jq}+\phi_{kr}-\phi_{ks})} \\ & + \sum_{p=1}^{M}\sum_{q=1}^{M}\sum_{r=1}^{M}\sum_{s=1}^{M}\sum_{j=1}^{N}\sum_{k\neq j}^{N}\sum_{l=1}^{N}\sum_{m\neq l} f_{jx} f^*_{ky} f_{lx} f^*_{my} h_p h^*_q h_r h^*_s \mathrm{e}^{\mathrm{i}(\phi_{jp}-\phi_{kq}+\phi_{lr}-\phi_{ms})} \\ & + \sum_{p=1}^{M}\sum_{q\neq p}^{M}\sum_{r=1}^{M}\sum_{s=1}^{M}\sum_{j=1}^{N}\sum_{k=1}^{N}\sum_{l\neq k}^{N} f_{jx} f^*_{jy} f_{kx} f^*_{ly} h_p h^*_q h_r h^*_s \mathrm{e}^{\mathrm{i}(\phi_{jp}-\phi_{jq}+\phi_{kr}-\phi_{ls})} \\ & + \sum_{p=1}^{M}\sum_{q=1}^{M}\sum_{r=1}^{M}\sum_{s\neq r}^{M}\sum_{j=1}^{N}\sum_{k\neq j}^{N}\sum_{l=1}^{N} f_{jx} f^*_{ky} f_{lx} f^*_{ly} h_p h^*_q h_r h^*_s \mathrm{e}^{\mathrm{i}(\phi_{jp}-\phi_{kq}+\phi_{lr}-\phi_{ls})}\ \mathrm{d}\phi^{N,M}. \end{aligned} \tag{C3}$$

These four summations originate from the square of the two summations in eq. (15). Only elements that are independent of all $\phi^{N,M}$ survive. For the first summation this implies that only elements for which $jp = ks$ and $jq = kr$ survive. Integration of the first summation hence gives $(2\pi)^{N\times M} \times M(M-1) \times \sum_{j=1}^{N} f_{jx} f^*_{jy} f_{jx} f^*_{jy}$. For the second summation, only elements for which $jp = ms$ and $kq = lr$ survive. Integration therefore results in $(2\pi)^{N\times M} \times M^2 \times \sum_{j=1}^{N}\sum_{k\neq j} f_{jx} f^*_{ky} f_{kx} f^*_{jy}$. The third and fourth summation contribute elements for which $jp = ls$ and $jq = kr$ and for which $jp = ls$ and $kq = lr$, respectively. Such elements do not exist and hence the expected values of these summations evaluate to zero. Consequently, $E[\hat{C}^{T\ 2}_{xyI}]$ is given by

$$E\left[\hat{C}^{T\ 2}_{xyI}\right] = \sum_{j=1}^{N}\sum_{k\neq j} f_{jx} f^*_{ky} f_{kx} f^*_{jy} + \sum_{j=1}^{N} f_{jx} f^*_{jy} f_{jx} f^*_{jy} - \frac{1}{M}\sum_{j=1}^{N} f_{jx} f^*_{jy} f_{jx} f^*_{jy}. \tag{C4}$$

The result in eq. (C4) can be applied to all products of incoherent terms by simply substituting x and y accordingly. We get for the expected values in eq. (C2), respectively:

$$E\left[\hat{C}^{T\ 2}_{xxI}\right] = \sum_{j=1}^{N}\sum_{k\neq j} f_{jx} f^*_{kx} f_{kx} f^*_{jx} + \left(1-\frac{1}{M}\right)\sum_{j=1}^{N} f_{jx} f^*_{jx} f_{jx} f^*_{jx}, \tag{C5}$$

$$E\left[\hat{C}^{T\ 2}_{yyI}\right] = \sum_{j=1}^{N}\sum_{k\neq j} f_{jy} f^*_{ky} f_{ky} f^*_{jy} + \left(1-\frac{1}{M}\right)\sum_{j=1}^{N} f_{jy} f^*_{jy} f_{jy} f^*_{jy}, \tag{C6}$$

$$E\left[\hat{C}^{T}_{xyI}\hat{C}^{T}_{xxI}\right] = \sum_{j=1}^{N}\sum_{k\neq j} f_{jx} f^*_{ky} f_{kx} f^*_{jx} + \left(1-\frac{1}{M}\right)\sum_{j=1}^{N} f_{jx} f^*_{jy} f_{jx} f^*_{jx}, \tag{C7}$$

$$E\left[\hat{C}^{T}_{xyI}\hat{C}^{T}_{yyI}\right] = \sum_{j=1}^{N}\sum_{k\neq j} f_{jx} f^*_{ky} f_{ky} f^*_{jy} + \left(1-\frac{1}{M}\right)\sum_{j=1}^{N} f_{jx} f^*_{jy} f_{jy} f^*_{jy} \tag{C8}$$

and

$$E\left[\hat{C}^{T}_{xxI}\hat{C}^{T}_{yyI}\right] = \sum_{j=1}^{N}\sum_{k\neq j} f_{jx} f^*_{kx} f_{ky} f^*_{jy} + \left(1-\frac{1}{M}\right)\sum_{j=1}^{N} f_{jx} f^*_{jx} f_{jy} f^*_{jy}. \tag{C9}$$

APPENDIX D: EXPLICIT COMPUTATION OF γ_{ap} FOR A HOMOGENOUS DISTRIBUTION OF FAR-FIELD SOURCES

In order to compute γ_{ap} explicitly, we need to solve for a specific distribution of sources. The result that is obtained in this appendix reveals that the second term on the right-hand side of each of the eqs (35)–(39) tends to be small with respect to the first term. That is to say, even for $M = 1$, we find that the corrections associated with the single integrals of products of four $f_{sx,\,y}$ are relatively small. This, combined with a good fit of our approximation to the numerically obtained behaviour of γ for an arbitrary distribution of sources in Section 4, justifies dropping these terms in our final approximation.

For simplicity, we assume a homogeneous distribution of far-field sources (see Fig. 1). Identical to Tsai (2011), we assume a constant $A_s = A$ along a circle with radius $R \gg r_{xy}$ centred between $\boldsymbol{x}$ and $\boldsymbol{y}$, where r_{xy} is the distance between the receivers at $\boldsymbol{x}$ and $\boldsymbol{y}$ (see Fig. D1). A_s is assumed zero for locations, $\boldsymbol{s}$, not situated on this circle. We define θ the azimuth of the source relative to the line connecting the receivers. For sources situated in the far field, the source–receiver distances r_{sx} and r_{sy} are accurately approximated by $R + \cos(\theta) r_{xy}/2$ and $R - \cos(\theta) r_{xy}/2$, respectively.

For the assumed distribution of far-field sources, we can safely assume the source–receiver distances large compared to the wavelength considered ($r_{sx} \gg c/\omega$). This allows us to approximate the Hankel function by (Arfken & Weber 2005),

$$H_0\left(\frac{r_{sx}\omega}{c}\right) \cong \sqrt{\frac{2c}{\pi r_{sx}\omega}}\,\mathrm{e}^{\mathrm{i}(r_{sx}\omega/c - \pi/4)}. \tag{D1}$$

We use this approximation and the geometrical approximations for r_{sx} and r_{sy} to calculate the integrals associated with the coherent terms, that is, eqs (32)–(34). We evaluate these integrals in Appendix E and recover the result of Tsai (2011) for ρ, that is, eq. (E1).

Eq. (29) shows that γ_{ap} is obtained by summing the expected values of γ_{ϵ^0}, γ_{ϵ^1} and γ_{ϵ^1} and subsequent multiplication by ρ. The expected values of the former two, that is, γ_{ϵ^0}, γ_{ϵ^1}, coincide with 1 and 0, respectively (see Appendix C). The expected value of γ_{ϵ^2} is obtained through solving eqs (35)–(39). These solutions are explicitly computed in Appendix F. We use the fact that $E[\hat{C}^{T\ 2}_{yyI}]$ coincides with $E[\hat{C}^{T\ 2}_{xxI}]$ and $\hat{C}^{2}_{yyC}$

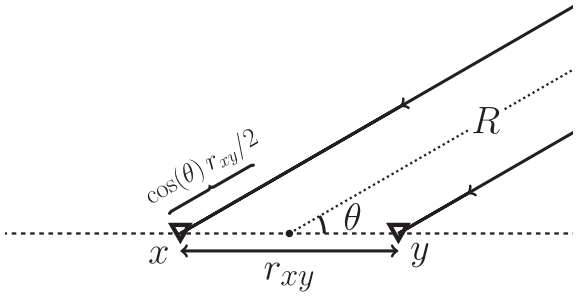

Figure D1. Receivers at x and y are separated a distance r_{xy}. Sources (not drawn) at distances R from the centre are sufficiently distant to assume the angle θ to be equal at $\boldsymbol{x}$ and $\boldsymbol{y}$ for an incoming wave.

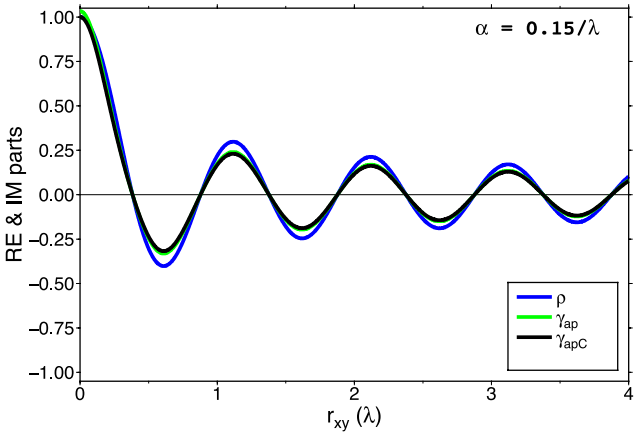

Figure D2. Behaviour of ρ (blue), $\gamma_{\rm ap}$ (green) and $\gamma_{\rm apC}$ (black) for sources randomly placed on a ring in the far field and an attenuation coefficient of $0.15/\lambda$. M is assumed to have a value of one. The green and black line display the behaviour of eq. (D3) with and without the last term, respectively.

with $\hat{C}^2_{xxC}$ and find:

$$E\left[\gamma_{\epsilon^2}\right] = E\left[\frac{3\hat{C}^{T\ 2}_{xxI}}{4\hat{C}^2_{xxC}} + \frac{\hat{C}^T_{xxI}\hat{C}^T_{yyI}}{4\hat{C}_{xxC}\hat{C}_{yyC}} - \frac{\hat{C}^T_{xyI}\hat{C}^T_{xxI}}{2\hat{C}_{xyC}\hat{C}_{xxC}} - \frac{\hat{C}^T_{xyI}\hat{C}^T_{yyI}}{2\hat{C}_{xyC}\hat{C}_{yyC}}\right]$$

$$\cong -\frac{1}{4} + \frac{1}{I_0^2\left(\alpha r_{xy}\right)}\left[\frac{1}{4}J_0^2\left(\frac{\omega r_{xy}}{c}\right) - \frac{3}{8\pi M}I_0\left(2\alpha r_{xy}\right) - \frac{1}{16\pi^2 M}\right]$$

$$+ \frac{1}{2\pi M\ J_0\left(\frac{\omega r_{xy}}{c}\right) \times I_0\left(\alpha r_{xy}\right)}\Re\left[J_0\left(\omega r_{xy}/c + \mathrm{i}\alpha r_{xy}\right)\right], \tag{D2}$$

where we use the relation $J_0(z) + J_0(z^*) = 2\Re[J_0(z)]$. Substituting this result and the expected values of γ_{ϵ^0} and γ_{ϵ^1} in expression (29), we obtain,

$$\gamma_{\rm ap} = \frac{3}{4\ I_0\left(\alpha r_{xy}\right)}J_0\left(\frac{\omega r_{xy}}{c}\right) + \frac{1}{4\ I_0^3\left(\alpha r_{xy}\right)}J_0^3\left(\frac{\omega r_{xy}}{c}\right)$$

$$+ \frac{1}{M}J_0\left(\frac{\omega r_{xy}}{c}\right)\left[\frac{\Re\left[J_0\left(\omega r_{xy}/c + i\alpha r_{xy}\right)\right]}{2\pi\ J_0\left(\frac{\omega r_{xy}}{c}\right) \times I_0^2\left(\alpha r_{xy}\right)} - \frac{3\ I_0\left(2\alpha r_{xy}\right)}{8\pi\ I_0^3\left(\alpha r_{xy}\right)} - \frac{1}{16\pi^2\ I_0^3\left(\alpha r_{xy}\right)}\right]. \tag{D3}$$

Note that this result is real and hence that $\Im[\gamma_{\rm ap}] = 0$ for all $\omega r_{xy}/c$ (with the operator $\Im[\ldots]$ mapping its complex argument into its imaginary part). Note that in the absence of attenuation, expression (D3) reduces to

$$\gamma_{\rm ap} = \frac{3}{4}J_0\left(\frac{\omega r_{xy}}{c}\right) + \frac{1}{4}J_0^3\left(\frac{\omega r_{xy}}{c}\right) + \frac{1}{M}\left(\frac{1}{2\pi} - \frac{3}{8\pi} - \frac{1}{16\pi^2}\right)J_0\left(\frac{\omega r_{xy}}{c}\right). \tag{D4}$$

The last term on the right-hand side of expression (D3) is small compared to the combined effect of the first two for all $\omega r_{xy}/c$. At $\omega r_{xy}/c = 0$ and for $M = 1$ it has a value of $\sim$0.033 and, due to the I_0^2 in the denominator, it also decays more rapidly with increasing $\omega r_{xy}/c$. In eq. (41) we introduce the 'coherent approximation', dubbed $\gamma_{\rm apC}$. It neglects the contribution of the single integrals in eqs (35)–(39) to the solution for $\gamma_{\rm ap}$. For our distribution of sources situated on a ring in the far field this implies that the last, lengthy term in (D3) is dropped. Fig. D2 presents the theoretical behaviour of ρ, $\gamma_{\rm ap}$ and $\gamma_{\rm apC}$ with M set to one.

From Appendix F we understand that the reason that the single integrals over the sources in eqs (35)–(39) only give small contributions is twofold. First, the double integrals result in a product of a sum of 2 (modified) Bessel functions, that is, a product of two coherent terms. The amplitude associated with this double integral term therefore includes a factor 4 (2^2). This factor is also included in the products of the coherent terms in the denominators of $E[\gamma_{\epsilon^2}]$, but is lacking in the result of the single integrals, which only evaluate to a single sum of two (modified) Bessel functions or no (modified) Bessel function at all. Second, a factor $1/\pi^2$ in the integrand of the single integrals further decreases the amplitude of this term. We find that the single integrals in eqs (35)–(38) only give contributions with an amplitude of $1/2\pi$ as can be seen in eqs (F7), (F9), (F12) and (F15), respectively. In case of $E[\hat{C}^T_{xxI}\hat{C}^T_{yyI}]$, which result is given by eq. (F18), only a $1/4\pi^2$ contribution of the single integral is found.

APPENDIX E: COMPUTATION OF C_{xyC}, C_{xxC} AND C_{yyC}

We use the approximation of the Hankel function in eq. (D1) and the geometrical approximations $r_{sx} \cong R + \cos(\theta)r_{xy}/2$ and $r_{sy} \cong R - \cos(\theta)r_{xy}/2$ (see Fig. D1) to compute explicitly the integrals in eqs (32)–(34). We assume a constant $A_s = A$. Using similar approximations

(i.e. a uniform distribution of far-field sources on a ring), Tsai (2011) explicitly calculates the time-domain coherent terms C_{xyC}, C_{xxC} and C_{yyC}. A subsequent Fourier decomposition gives him the following approximation for ρ:

$$\rho(\omega, r_{xy}) = \frac{1}{I_0\left(\alpha r_{xy}\right)} J_0\left(\frac{\omega r_{xy}}{c}\right), \tag{E1}$$

where I_0 denotes a 0-th order modified Bessel function of the first kind (henceforth modified Bessel function).

Substituting the Hankel function approximation in the expression for f_{sx}, that is, eq. (31), and subsequently substituting the approximations for r_{sx} and r_{xy}, we get,

$$\begin{aligned}
\hat{C}_{xyC} &= \int_S f_{sx} f_{sy}^* \, \mathrm{d}\boldsymbol{s} \\
&\cong \frac{cA^2}{8\pi\omega} \int_0^{2\pi} \frac{\mathrm{e}^{-2\alpha R}/R}{\sqrt{1 - \frac{\cos^2(\theta) r_{xy}^2}{4R^2}}} \, \mathrm{e}^{\mathrm{i}\omega\cos(\theta) r_{xy}/c} \, \mathrm{d}\theta \\
&\cong \frac{cA^2 e^{-2\alpha R}}{8\pi\omega R} \int_0^{2\pi} e^{i\omega\cos(\theta) r_{xy}/c} \, \mathrm{d}\theta \\
&= \frac{cA^2 e^{-2\alpha R}}{4\omega R} J_0\left(\frac{\omega r_{xy}}{c}\right),
\end{aligned} \tag{E2}$$

where we have recognized an integral expression of the Bessel function [eq. (11.30c) of Arfken & Weber (2005)]. We have neglected $\cos^2(\theta) r_{xy}^2/4R^2$ in the denominator, because we assume $R \gg r_{xy}$. Similarly, C_{xxC} is approximated by

$$\begin{aligned}
\hat{C}_{xxC} &= \int_S f_{sx} f_{sx}^* \, \mathrm{d}\boldsymbol{s} \\
&\cong \frac{cA^2}{8\pi\omega} \int_0^{2\pi} \frac{\mathrm{e}^{-\alpha\left[2R + \cos(\theta) r_{xy}\right]}/R}{1 + \frac{\cos(\theta) r_{xy}}{2R}} \, \mathrm{d}\theta \\
&\cong \frac{cA^2 \mathrm{e}^{-2\alpha R}}{8\pi\omega R} \int_0^{2\pi} \mathrm{e}^{-\alpha\cos(\theta) r_{xy}} \, \mathrm{d}\theta \\
&= \frac{cA^2 \mathrm{e}^{-2\alpha R}}{4\omega R} I_0\left(\alpha r_{xy}\right),
\end{aligned} \tag{E3}$$

where we have made use of the fact that the cosine function is an even function around π and hence recognized two integral expressions of the modified Bessel function [eq. (9.6.16) of Abramowitz & Stegun (1964)]. We have neglected $\cos(\theta) r_{xy}/2R$ in the denominator, because we assume $R \gg r_{xy}$. Following the same procedure we find for C_{yyC},

$$\hat{C}_{yyC} \cong \frac{cA^2 \mathrm{e}^{-2\alpha R}}{4\omega R} I_0\left(\alpha r_{xy}\right). \tag{E4}$$

Substituting the computed $\hat{C}_{xyC}$, $\hat{C}_{xxC}$ and $\hat{C}_{yyC}$ in eq. (22), we recover the expression for ρ obtained by Tsai (2011), that is, eq. (E1).

APPENDIX F: COMPUTATION OF THE TERMS OF THE EXPECTED VALUE OF γ_{ϵ^2}

Using again the approximation of the Hankel function in eq. (D1) and the geometrical approximations $r_{sx} \cong R + \cos(\theta) r_{xy}/2$ and $r_{sy} \cong R - \cos(\theta) r_{xy}/2$ (see Fig. D1), we solve the integrals in eqs (35)–(39). While the corrections associated with the single integrals of products of four $f_{sx,y}$ contain squares of $f_{sx,y}$ and $f_{sx,y}^*$, we first calculate these separately. The obtained expressions are substituted when evaluating the single integrals to give:

$$\begin{aligned}
f_{sx}^2 &= \left[\frac{\mathrm{i}}{4} A H_0\left(\frac{r_{sx}\omega}{c}\right) \mathrm{e}^{-\alpha r_{sx}}\right]^2 \\
&\cong \frac{-cA^2}{8\pi\omega r_{sx}} \mathrm{e}^{-2\alpha r_{sx}} \mathrm{e}^{\mathrm{i}(2r_{sx}\omega/c - \pi/2)},
\end{aligned} \tag{F1}$$

$$\begin{aligned}
f_{sx}^{*2} &= \left[\frac{-\mathrm{i}}{4} A H_0^*\left(\frac{r_{sx}\omega}{c}\right) \mathrm{e}^{-\alpha r_{sx}}\right]^2 \\
&\cong \frac{-cA^2}{8\pi\omega r_{sx}} \mathrm{e}^{-2\alpha r_{sx}} \mathrm{e}^{-\mathrm{i}(2r_{sx}\omega/c - \pi/2)},
\end{aligned} \tag{F2}$$

$$f_{sy}^2 = \left[\frac{\mathrm{i}}{4} A H_0\left(\frac{r_{sy}\omega}{c}\right)\mathrm{e}^{-\alpha r_{sy}}\right]^2$$
$$\cong \frac{-cA^2}{8\pi\omega r_{sy}}\mathrm{e}^{-2\alpha r_{sy}}\mathrm{e}^{\mathrm{i}\left(2r_{sy}\omega/c-\pi/2\right)}, \tag{F3}$$

$$f_{sy}^{*2} = \left[\frac{-\mathrm{i}}{4} A H_0^*\left(\frac{r_{sy}\omega}{c}\right)\mathrm{e}^{-\alpha r_{sy}}\right]^2$$
$$\cong \frac{-cA^2}{8\pi\omega r_{sy}}\mathrm{e}^{-2\alpha r_{sy}}\mathrm{e}^{-\mathrm{i}\left(2r_{sy}\omega/c-\pi/2\right)}. \tag{F4}$$

In order to calculate the incoherent terms we write the double integral over sources as the product of two integrals. We subsequently substitute the appropriate coherent terms [eq. (E2), (E3) or (E4), or a combination of these]. For $E[\hat{C}_{xxI}^{T\ 2}]$, that is, eq. (35), we get,

$$E\left[\hat{C}_{xxI}^{T\ 2}\right] = \int_S f_{sx} f_{sx}^*\,\mathrm{d}\boldsymbol{s} \times \int_S f_{s'x}^* f_{s'x}\,\mathrm{d}\boldsymbol{s}' - \frac{1}{M}\int_S f_{sx}^2 f_{sx}^{*2}\,\mathrm{d}\boldsymbol{s}$$
$$\cong \left[\frac{cA^2\mathrm{e}^{-2\alpha R}}{4\omega R}\, I_0\left(\alpha r_{xy}\right)\right]^2 - \frac{1}{M}\int_S f_{sx}^2 f_{sx}^{*2}\,\mathrm{d}\boldsymbol{s}. \tag{F5}$$

We use eqs (F1) and (F2) and approximate the integral of $f_{sx}^2 f_{sx}^{*2}$,

$$\int_S f_{sx}^2 f_{sx}^{*2}\,\mathrm{d}\boldsymbol{s} \cong \frac{c^2A^4}{64\pi^2\omega^2}\int_0^{2\pi}\frac{\mathrm{e}^{-4\alpha\left[R+\cos(\theta)r_{xy}/2\right]}}{\left[R+\frac{\cos(\theta)r_{xy}}{2}\right]^2}\,\mathrm{d}\theta$$
$$= \frac{c^2A^4}{64\pi^2\omega^2}\mathrm{e}^{-4\alpha R}\int_0^{2\pi}\frac{\mathrm{e}^{-2\alpha\cos(\theta)r_{xy}}/R^2}{1+\frac{\cos(\theta)r_{xy}}{R}+\frac{\cos^2(\theta)r_{xy}^2}{R^2}}\,\mathrm{d}\theta$$
$$\cong \frac{c^2A^4}{64\pi^2\omega^2}\frac{\mathrm{e}^{-4\alpha R}}{R^2}\int_0^{2\pi}\mathrm{e}^{-2\alpha\cos(\theta)r_{xy}}\,\mathrm{d}\theta$$
$$= \frac{c^2A^4\mathrm{e}^{-4\alpha R}}{32\pi\omega^2R^2}\, I_0\left(2\alpha r_{xy}\right), \tag{F6}$$

where we have made use of the fact that the cosine function is an even function around π and hence recognized two integral expressions of the modified Bessel function [eq. (9.6.16) of Abramowitz & Stegun (1964)]. We have neglected $\cos(\theta)r_{xy}/R + \cos^2(\theta)r_{xy}^2/R^2$ in the denominator, because we assume $R \gg r_{xy}$. Substituting this expression in eq. (F5) we arrive at,

$$E\left[\hat{C}_{xxI}^{T\ 2}\right] \cong \frac{c^2A^4\mathrm{e}^{-4\alpha R}}{16\omega^2R^2}\left[\, I_0^2\left(\alpha r_{xy}\right) - \frac{1}{2\pi M} I_0\left(2\alpha r_{xy}\right)\right]. \tag{F7}$$

The integral of $f_{sy}^2 f_{sy}^{*2}$ gives an identical result to the one of $f_{sx}^2 f_{sx}^{*2}$ although we neglect $-\cos(\theta)r_{xy}/R + \cos^2(\theta)r_{xy}^2/R^2$ in the denominator in this case, that is,

$$\int_S f_{sy}^2 f_{sy}^{*2}\,\mathrm{d}\boldsymbol{s} \cong \frac{c^2A^4}{64\pi^2\omega^2}\int_0^{2\pi}\frac{\mathrm{e}^{-4\alpha\left[R-\cos(\theta)r_{xy}/2\right]}}{\left[R-\frac{\cos(\theta)r_{xy}}{2}\right]^2}\,\mathrm{d}\theta$$
$$= \frac{c^2A^4}{64\pi^2\omega^2}\mathrm{e}^{-4\alpha R}\int_0^{2\pi}\frac{\mathrm{e}^{2\alpha\cos(\theta)r_{xy}}/R^2}{1-\frac{\cos(\theta)r_{xy}}{R}+\frac{\cos^2(\theta)r_{xy}^2}{R^2}}\,\mathrm{d}\theta$$
$$\cong \frac{c^2A^4}{64\pi^2\omega^2}\frac{\mathrm{e}^{-4\alpha R}}{R^2}\int_0^{2\pi}\mathrm{e}^{2\alpha\cos(\theta)r_{xy}}\,\mathrm{d}\theta$$
$$= \frac{c^2A^4\mathrm{e}^{-4\alpha R}}{32\pi\omega^2R^2}\, I_0\left(2\alpha r_{xy}\right). \tag{F8}$$

For $E[\hat{C}^{T\ 2}_{yyI}]$, that is, eq. (36), we therefore obtain,

$$\begin{aligned} E\left[\hat{C}^{T\ 2}_{yyI}\right] &= \int_S f_{sy} f^*_{sy}\,\mathrm{d}\boldsymbol{s} \times \int_S f^*_{s'y} f_{s'y}\mathrm{d}\boldsymbol{s}' - \frac{1}{M}\int_S f^2_{sy} f^{*2}_{sy}\,\mathrm{d}\boldsymbol{s} \\ &\cong \left[\frac{cA^2\mathrm{e}^{-2\alpha R}}{4\omega R}\, I_0\left(\alpha r_{xy}\right)\right]^2 - \frac{c^2A^4\mathrm{e}^{-4\alpha R}}{32\pi\omega^2R^2M}\, I_0\left(2\alpha r_{xy}\right) \\ &= \frac{c^2A^4\mathrm{e}^{-4\alpha R}}{16\omega^2R^2}\left[\, I_0^2\left(\alpha r_{xy}\right) - \frac{1}{2\pi M} I_0\left(2\alpha r_{xy}\right)\right]. \end{aligned} \tag{F9}$$

We calculate $E[\hat{C}^T_{xyI}\hat{C}^T_{xxI}]$, that is, eq. (37), substituting the result for $\hat{C}_{xyC}$ and $\hat{C}_{xxC}$,

$$\begin{aligned} E\left[\hat{C}^T_{xyI}\hat{C}^T_{xxI}\right] &= \int_S f_{sx} f^*_{sy}\,\mathrm{d}\boldsymbol{s} \times \int_S f_{s'x} f^*_{s'x}\mathrm{d}\boldsymbol{s}' - \frac{1}{M}\int_S f^2_{sx} f^*_{sx} f^*_{sy}\,\mathrm{d}\boldsymbol{s} \\ &\cong \frac{c^2A^4\mathrm{e}^{-4\alpha R}}{16\omega^2R^2}\left[J_0\left(\frac{\omega r_{xy}}{c}\right) \times I_0\left(\alpha r_{xy}\right)\right] - \frac{1}{M}\int_S f^2_{sx} f^*_{sx} f^*_{sy}\,\mathrm{d}\boldsymbol{s}. \end{aligned} \tag{F10}$$

We use (F1) and approximate the integral $\int_S f^2_{sx} f^*_{sx} f^*_{sy}\,\mathrm{d}\boldsymbol{s}$,

$$\begin{aligned} \int_S f^2_{sx} f^*_{sx} f^*_{sy}\,\mathrm{d}\boldsymbol{s} &\cong \frac{c^2A^4}{64\pi^2\omega^2}\int_0^{2\pi} \frac{\mathrm{e}^{-\alpha\left[4R+\cos(\theta)r_{xy}\right]}}{\left[R+\frac{\cos(\theta)r_{xy}}{2}\right]\sqrt{\left[R^2-\frac{\cos^2(\theta)r^2_{xy}}{4}\right]}}\,\mathrm{e}^{\mathrm{i}\omega r_{xy}\cos(\theta)/c}\,\mathrm{d}\theta \\ &= \frac{c^2A^4}{64\pi^2\omega^2}\int_0^{2\pi} \frac{\mathrm{e}^{-\alpha\left[4R+\cos(\theta)r_{xy}\right]}/R}{\left[1+\frac{\cos(\theta)r_{xy}}{2R}\right]\sqrt{\left[1-\frac{\cos^2(\theta)r^2_{xy}}{4R^2}\right]}}\,\mathrm{e}^{\mathrm{i}\omega r_{xy}\cos(\theta)/c}\,\mathrm{d}\theta \\ &\cong \frac{c^2A^4\mathrm{e}^{-4\alpha R}}{64\pi^2\omega^2R^2}\int_0^{2\pi}\mathrm{e}^{\mathrm{i}\cos(\theta)\left[\omega r_{xy}/c+\mathrm{i}\alpha r_{xy}\right]}\,\mathrm{d}\theta \\ &= \frac{c^2A^4\mathrm{e}^{-4\alpha R}}{32\pi\omega^2R^2}J_0\left(\omega r_{xy}/c+\mathrm{i}\alpha r_{xy}\right), \end{aligned} \tag{F11}$$

where we have approximated $[1+\cos(\theta)\,r_{xy}/2R]\sqrt{\left[1-\cos^2(\theta)\,r^2_{xy}/4R^2\right]} \cong 1$ in the denominator and recognized an integral expression of the Bessel function [eq. (11.30c) of Arfken & Weber (2005)]. We arrive at

$$E\left[\hat{C}^T_{xyI}\hat{C}^T_{xxI}\right] \cong \frac{c^2A^4\mathrm{e}^{-4\alpha R}}{16\omega^2R^2}\left[J_0\left(\frac{\omega r_{xy}}{c}\right) I_0\left(\alpha r_{xy}\right) \;-\; \frac{1}{2\pi M}J_0\left(\omega r_{xy}/c+\mathrm{i}\alpha r_{xy}\right)\right]. \tag{F12}$$

The expression for $E[\hat{C}^T_{xyI}\hat{C}^T_{yyI}]$, that is, eq. (38), can be obtained in a similar way,

$$\begin{aligned} E\left[\hat{C}^T_{xyI}\hat{C}^T_{yyI}\right] &= \int_S f_{sx} f^*_{sy}\,\mathrm{d}\boldsymbol{s} \times \int_S f_{s'y} f^*_{s'y}\mathrm{d}\boldsymbol{s}' - \frac{1}{M}\int_S f^{*2}_{sy} f_{sx} f_{sy}\,\mathrm{d}\boldsymbol{s} \\ &\cong \frac{c^2A^4\mathrm{e}^{-4\alpha R}}{16\omega^2R^2}\left[J_0\left(\frac{\omega r_{xy}}{c}\right) \times I_0\left(\alpha r_{xy}\right)\right] - \frac{1}{M}\int_S f^{*2}_{sy} f_{sx} f_{sy}\,\mathrm{d}\boldsymbol{s}, \end{aligned} \tag{F13}$$

where we have simply substituted the result for $\hat{C}_{xyC}$ and $\hat{C}_{yyC}$. We use (F4) and approximate the integral $\int_S f^{*2}_{sy} f_{sx} f_{sy}\,\mathrm{d}\boldsymbol{s}$,

$$\begin{aligned} \int_S f^{*2}_{sy} f_{sx} f_{sy}\,\mathrm{d}\boldsymbol{s} &\cong \frac{c^2A^4}{64\pi^2\omega^2}\int_0^{2\pi} \frac{\mathrm{e}^{-\alpha\left[4R-\cos(\theta)r_{xy}\right]}}{\left[R-\frac{\cos(\theta)r_{xy}}{2}\right]\sqrt{\left[R^2-\frac{\cos^2(\theta)r^2_{xy}}{4}\right]}}\,\mathrm{e}^{\mathrm{i}\omega r_{xy}\cos(\theta)/c}\,\mathrm{d}\theta \\ &= \frac{c^2A^4}{64\pi^2\omega^2}\int_0^{2\pi} \frac{\mathrm{e}^{-\alpha\left[4R-\cos(\theta)r_{xy}\right]}/R}{\left[1-\frac{\cos(\theta)r_{xy}}{2R}\right]\sqrt{\left[1-\frac{\cos^2(\theta)r^2_{xy}}{4R^2}\right]}}\,\mathrm{e}^{\mathrm{i}\omega r_{xy}\cos(\theta)/c}\,\mathrm{d}\theta \\ &\cong \frac{c^2A^4\mathrm{e}^{-4\alpha R}}{64\pi^2\omega^2R^2}\int_0^{2\pi}\mathrm{e}^{\mathrm{i}\cos(\theta)\left[\omega r_{xy}/c-\mathrm{i}\alpha r_{xy}\right]}\,\mathrm{d}\theta \\ &= \frac{c^2A^4\mathrm{e}^{-4\alpha R}}{32\pi\omega^2R^2}J_0\left(\omega r_{xy}/c-\mathrm{i}\alpha r_{xy}\right), \end{aligned} \tag{F14}$$

where we have approximated $\left[1-\cos(\theta)r_{xy}/2R\right]\sqrt{\left[1-\cos^2(\theta)r_{xy}^2/4R^2\right]} \cong 1$ in the denominator. Substituting the result in eq. (F13), we obtain

$$E\left[\hat{C}^T_{xyI}\hat{C}^T_{yyI}\right] \cong \frac{c^2A^4\mathrm{e}^{-4\alpha R}}{16\omega^2R^2}\left[J_0\left(\frac{\omega r_{xy}}{c}\right)I_0\left(\alpha r_{xy}\right) - \frac{1}{2\pi M}J_0\left(\omega r_{xy}/c - \mathrm{i}\alpha r_{xy}\right)\right]. \tag{F15}$$

We finally compute eq. (39), that is,

$$\begin{aligned} E\left[\hat{C}^T_{xxI}\hat{C}^T_{yyI}\right] &= \int_S f_{sx}f^*_{sy}\,\mathrm{d}\boldsymbol{s}\times\int_S f_{s'y}f^*_{s'x}\mathrm{d}\boldsymbol{s}' - \frac{1}{M}\int_S f_{sx}f^*_{sx}f_{sy}f^*_{sy}\,\mathrm{d}\boldsymbol{s} \\ &\cong \frac{c^2A^4\mathrm{e}^{-4\alpha R}}{16\omega^2R^2}\,J_0^2\left(\frac{\omega r_{xy}}{c}\right) - \frac{1}{M}\int_S f_{sx}f^*_{sx}f_{sy}f^*_{sy}\,\mathrm{d}\boldsymbol{s}, \end{aligned} \tag{F16}$$

where we have used the fact that $\hat{C}_{yxC} = \hat{C}_{xyC}$ and hence substituted the results for $\hat{C}_{xyC}$. We compute the second term,

$$\begin{aligned} \int_S f_{sx}f^*_{sx}f_{sy}f^*_{sy}\,\mathrm{d}\boldsymbol{s} &\cong \frac{A^2}{16}\mathrm{e}^{-2\alpha r_{sx}}\frac{2c}{\pi r_{sx}\omega}\,\mathrm{e}^{\mathrm{i}[(r_{sx}\omega/c-\pi/4)-(r_{sx}\omega/c-\pi/4)]} \\ &\quad\times\frac{A^2}{16}\mathrm{e}^{-2\alpha r_{sy}}\frac{2c}{\pi r_{sy}\omega}\,\mathrm{e}^{\mathrm{i}[(r_{sy}\omega/c-\pi/4)-(r_{sy}\omega/c-\pi/4)]} \\ &\cong \frac{c^2A^4\mathrm{e}^{-4\alpha R}}{64\pi^2\omega^2R^2}, \end{aligned} \tag{F17}$$

and substitute this in eq. (F16) to find

$$E\left[\hat{C}^T_{xxI}\hat{C}^T_{yyI}\right] \cong \frac{c^2A^4\mathrm{e}^{-4\alpha R}}{16\omega^2R^2}\left[J_0^2\left(\frac{\omega r_{xy}}{c}\right) - \frac{1}{4\pi^2M}\right]. \tag{F18}$$